



# On the relevance of the electron density analysis for the study of microhydration and its impact on the formation of a peptide-like bond

Imene Derbali, Olivier Aroule, Guillaume Hoffmann, R. Thissen, Christian Alcaraz, Claire Romanzin, Emilie-Laure Zins

## ► To cite this version:

Imene Derbali, Olivier Aroule, Guillaume Hoffmann, R. Thissen, Christian Alcaraz, et al.. On the relevance of the electron density analysis for the study of microhydration and its impact on the formation of a peptide-like bond. Theoretical Chemistry Accounts: Theory, Computation, and Modeling, 2022, 10.1007/s00214-022-02893-7 . hal-03719937

**HAL Id: hal-03719937**

**<https://hal.science/hal-03719937v1>**

Submitted on 11 Jul 2022

**HAL** is a multi-disciplinary open access archive for the deposit and dissemination of scientific research documents, whether they are published or not. The documents may come from teaching and research institutions in France or abroad, or from public or private research centers.

L'archive ouverte pluridisciplinaire **HAL**, est destinée au dépôt et à la diffusion de documents scientifiques de niveau recherche, publiés ou non, émanant des établissements d'enseignement et de recherche français ou étrangers, des laboratoires publics ou privés.

# On the relevance of the electron density analysis for the study of micro-hydration and its impact on the formation of a peptide-like bond

Imene Derbali,<sup>a</sup> Olivier Aroule,<sup>a</sup> Guillaume Hoffmann,<sup>a</sup> Roland Thissen,<sup>b,c</sup> Christian Alcaraz,<sup>b,c</sup> Claire Romanzin,<sup>b,c</sup> Emilie-Laure Zins<sup>a\*</sup>

a: Sorbonne Université, CNRS, De la Molécule aux Nano-Objets: Réactivité, Interactions Spectroscopies, MONARIS, 75005, Paris, France

b: Institut de Chimie Physique, Bât. 350, UMR 8000, CNRS-Univ. Paris Saclay, Orsay, France

c: Synchrotron SOLEIL, L'Orme des Merisiers, Saint-Aubin—BP 48, Gif-sur-Yvette, France

\*: Corresponding author, emilie-laure.zins@sorbonne-universite.fr, ORCID 0000-0002-2157-6696

## Abstract

The formation of a peptide bond from carboxylic acid and amine from the reactants taken separately in the gas phase with no catalytic surface constitutes an interesting process from an exobiological point of view. We investigated the reaction between acetic acid ( $\text{CH}_3\text{-COOH}$ ) and methylamine ( $\text{CH}_3\text{-NH}_2$ ), alone and with the presence of one to five water molecules, at the LC- $\omega$ PBE/6-311++G(d,p) level of theory, with the GD3BJ Empirical Dispersion. Starting from the idea that the reaction begins with the formation of a non-covalent complex between the reagents, we first identified the main structures of non-covalent complexes that can be formed between both reagents without hydration, by maximizing interactions between complementary sites of both partners. This study led to the identification of a ( $\text{CH}_3\text{-COOH}$ ):( $\text{CH}_3\text{-NH}_2$ ) complex, with a stabilization energy of 14.22 kJ/mol, that may correspond to a preliminary step towards the formation of a peptide-like bond.

## Introduction

The role played by a few water molecules in the reaction leading to the formation of a C-N peptide bond has been the subject of several pioneering studies in recent years. In particular, the reaction mechanisms of prebiotic interest, even those involving particularly simple precursors, have been studied with and without explicit few water molecules, in the gas phase using quantum chemistry approaches.<sup>1,2,3</sup> In a thorough study dedicated to the Strecker synthesis of glycine from ammonia and formaldehyde,<sup>4</sup> Riffet, Frison and Bouchoux showed that water molecules may interact as hydrogen-bond donors and hydrogen-bond acceptors without being directly impacted in the reaction: such interactions were referred to as "passive catalysis". Alternatively, water molecules may form a "bridge" or a hydrogen bonding network between a hydrogen atom bounded to ammonia and the oxygen atom of formaldehyde: such interactions were referred to as "active catalysis". The authors studied this reaction with 0 - 4 water molecules. Without any water molecules, the reaction is calculated to be endothermic with an energy barrier of 133 kJ/mol at the G3B3 level of theory, and the authors demonstrated that the reaction becomes barrierless in the presence of 3 water molecules acting as "active catalysis". In this study, the authors also demonstrated that the reaction begins with the formation of a non-covalent complex. When the reaction occurs with no water molecule, the C=O bond of formaldehyde and one of the N-H bonds of ammonia are located in parallel planes. A similar "four-ring" structure was also identified in the non-covalent complexes leading to the reactions of  $R_aR_bNH$  and  $HCO(CH_2R')$  with  $R_a, R_b = H$  or  $CH_3$  and  $R' = H, OH$  or  $OOH$ .<sup>1,2,3</sup>

Moreover, the study of such reaction mechanisms would also allow to better describe the formation of atmospheric aerosols as well as atmospherically-relevant reactions,<sup>5-9</sup> the formation of prebiotic molecules in hot-cores, hot-corinos<sup>10</sup> and in complex environments,<sup>11-16</sup> as well as to contribute to more fundamental studies on reactivity<sup>17</sup>.

Besides, several methodological approaches have been proposed to theoretically identify microhydrated isomers. [Table 1](#) presents three types of approaches, all of which are commonly applied today:

- a phenomenological approach, mainly based on the identification of complementary reaction sites from the fundamental equations of quantum chemistry,
- a stochastic approach derived from semi-classical calculations,
- an approach based on similarity of interactions for given functional groups.

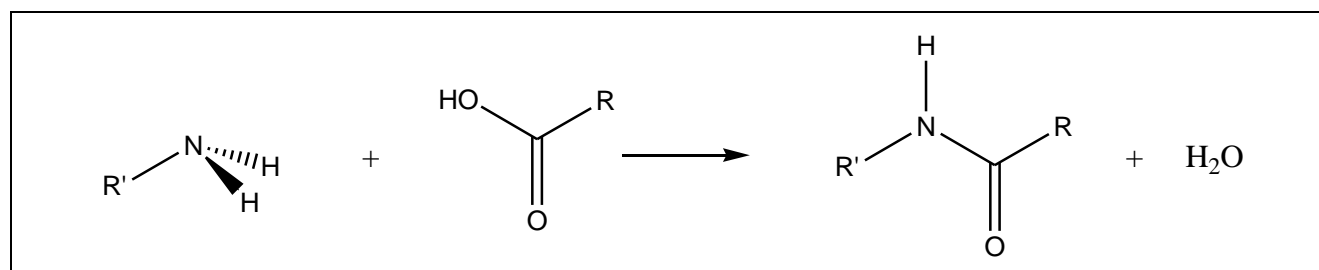
Regarding the phenomenological approach, different chemical reactivity descriptors have been developed to rationalize the reaction mechanisms and the propensity of different chemical species to interact and react. Approaches based on the study of electrostatic potentials allow the identification of electrophilic and nucleophilic sites. These approaches are particularly relevant for the study of processes under charge control. In a complementary way, the descriptors of the conceptual DFT have been developed since the end of the 1980s to describe and understand the propensity of chemical species to react or interact.<sup>18</sup> Among the descriptors of the conceptual DFT, the Fukui functions allow to evaluate the influence of the addition or the cession of an electron on a chemical system, from an orbital viewpoint.<sup>19, 20</sup>

Types of approach	Exemple of development or of application
Phenomenological	Politzer et al.: interactions between the most electrophilic and the most nucleophilic sites <sup>21-27</sup> Gadre et al.: Electrostatic Potential for Intermolecular Complexation model <sup>28-32</sup> Conceptual DFT: Parr, Yang, Toro-Labbé, Ayers, De Proft, Geerlings, Morell et al. <sup>18-20,33-35</sup>
Stochastic	Bouchoux, <sup>4</sup> Bacchus <sup>36</sup> et al.
Similarity of interactions for given functional groups	Alonso, <sup>37</sup> Blanco, <sup>38</sup> Schnell <sup>39</sup> et al.

**Table 1: Comparison of three types of approaches used to theoretically search for microhydrated complexes.**

It should be noticed that it is always difficult to identify the most relevant reaction paths. Also, it is always tricky, in the search for non-covalent complexes, to identify with certainty the most stable structures. Moreover, investigating the formation of covalent bonds and weak, non-covalent bonds in the same study represents an additional methodological challenge. A unified methodology for the investigation of the reaction path and microhydration would be a major step ahead.

All these aspects will be presented in the present study. For this purpose, we have selected a particularly simple prototype reaction: the formation of a peptide-like bond between acetic acid and methylamine, in the presence of 0 to 5 molecules of water ([Scheme 1](#)).



**Scheme 1: Reactions of the peptide bond formation between a carboxylic acid and an amine.**

The formation of such a peptide-like bond was experimentally observed between ionized acetic acid and methylamine taken separately and close to their fundamental state.<sup>40</sup> Because of the prebiotic and exobiological interest of this reaction,<sup>41,42,43</sup> it seems necessary to deepen the research on this kind of reaction, starting from neutral or ionized reagents, especially by determining the role that some water molecules could play on the reaction. Water plays indeed a major role in the chemistry of the interstellar medium.<sup>44,45,46</sup> The aim of this work is to identify theoretically the reaction pathways associated with the formation of a peptide-like bond between acetic acid and methylamine, in the presence of some explicit water molecules.

Our methodological approach is based on the identification of complementary sites of interaction on partners, and on the maximization of interactions between complementary sites. This approach is in line with the studies of Politzer and Muray:<sup>47</sup> the anisotropy of electron distribution around some

atoms can be determined by calculating the electrostatic potential  $V(r)$  generated at any point in the space by electrons and nuclei:

$$V(\vec{r}) = \sum_A \frac{Z_A}{|\vec{R}_A - \vec{r}|} - \int \frac{\rho(\vec{r}')}{|\vec{r}' - \vec{r}|} d\vec{r}' \quad (1)$$

The contributions of the nuclei are gathered in the first term of the equation, with  $Z_A$  being the charge of nucleus A located in  $\vec{R}_A$ . The second term takes into account the total charge distribution of the electrons, and the term  $\rho(r)$  represents the electron density of the molecule.

$V(r)$  is usually plotted on a "surface" of the molecule. This is referred to as molecular electrostatic potential (MESP). Following Bader's suggestion, the MESP is usually computed on an isosurface with an electron density of  $0.001 \text{ e.bohr}^{-3}$ . This isosurface is considered to generally encompass more than 95% of the charge of the system, and to fit with the surface of the molecule,<sup>48</sup> and is often considered as the surface of the molecule.<sup>48</sup> The MESP plotted on this surface would thus correspond to the electrostatic potential experienced by the surrounding species.

The relevance of using MESP for the identification of interactions between polar molecules has been demonstrated many times in literature.<sup>21-27</sup> However, it should be noticed that some debates are still going on in the literature regarding the relevance of using MESP for interactions of a dispersive nature (in particular benzene dimer, or halide anion and water molecule).<sup>49,50</sup>

Gadre and Pundlik<sup>28-32</sup> recommend the use of topological analysis of  $V(r)$  to identify the formation of non-covalent complexes while avoiding geometry optimization calculations: in their model (Electrostatic Potential for Intermolecular Complexation, EPIC), the optimal geometry of a complex as well as the interaction energy are determined from the isolated partners.

Alternatively, and in line with the work of Clark, Politzer and Murray, several teams rely on a detailed analysis of the MESP to interpret the non-covalent interactions formed in between two (or more) partners. A Quantitative structure-activity relationship (QSAR) approach based on MESP analysis has also been developed.<sup>53-55</sup>

In this work, we will show how the analysis of the MESP of isolated partners allows the identification of a complex that may constitute a preliminary step in the reaction of peptide-like bond formation between  $\text{CH}_3\text{COOH}$  and  $\text{NH}_2\text{CH}_3$ . We will then present how a similar methodological approach allows the identification of reaction pathways in the presence of one to five water molecules. Finally, the influence of one to five water molecules on reactivity will be studied.

For comparative purposes, the use of Fukui functions and the Dual Descriptor from the conceptual DFT will also be considered.

## Method

All the calculations were performed with the Gaussain09 software (revision D.01).<sup>56</sup>

The reaction paths investigated in this paper involve the formation of non-covalent interactions. The level of calculation should therefore be carefully chosen to correctly describe these interactions. Moreover, this study requires considering many stationary points as well as intrinsic reaction coordinates (IRC) calculations. This is why we have chosen the DFT with the range separated LC- $\omega$ PBE<sup>57-59</sup> functional, in combination with the empirical correction GD3BJ proposed by Becke and

Johnson, and formalized by Grimme<sup>60</sup>, and with the triple  $\zeta$  Pople basis 6-311++G(d,p).<sup>61</sup> The relevance of such a level of calculation for the type of complexes herein considered has been previously benchmarked by Grimme et al. and Dilabio et al.<sup>62,63</sup>

A ultrafine integration grid was used together with a tight convergence criterion for geometry optimizations. For all the structures herein considered, the total geometry optimizations were systematically completed by frequency calculations, in order to identify the transition states of the reaction intermediates. IRC calculations (forward and reverse) were performed on all structures identified as transition states.

The "wfn" files needed for topological characterization were generated during this step. All the MESP's were obtained by plotting the total electrostatic potential on an electronic isodensity surface of 0.001 e-bohr<sup>-3</sup>, using the AIMAll package. Furthermore, for optimized complexes and transition states, a topological characterization of the non-covalent interactions based on the QTAIM approach<sup>64</sup> was performed using the AIMAll package.

In this work, QTAIM analysis will be mainly used to identify non-covalent interactions (in particular hydrogen bonding interactions between water molecules and a polar molecule: acetic acid, methylamine, methylacetamide) via the presence of critical bonding points. Although based on a fundamental quantity of quantum physics, namely the electron density, the analysis of BCP to investigate some non-covalent interactions has been criticized in the literature. In some cases, these BCPs are found to be the consequence of artifacts or of the Poincaré-Hopf relationship.<sup>65,66,67</sup>

However, it should be noticed that in the case of "simple" hydrogen bonding interactions, such as those studied in the present article, the BCP allow to highlight non-covalent interactions.<sup>68-79</sup>

DFT calculations still remain the most appropriate approach when searching for reaction paths involving multiple non-covalent interactions between multiple partners. The choice of the level of calculation is crucial to the quality of the results obtained. The choice of the LC- $\omega$ PBE/6-31++G(d,p) in combination with the GD3BJ Grimme empirical correction was previously validated on rotational constants and IR spectra for the identification of microhydrated complexes with R<sub>2</sub>CO, (CH<sub>3</sub>)<sub>3</sub>NO and CH<sub>3</sub>COCOCOCH<sub>3</sub>.

For the identification of non-covalent complexes and reaction pathways by quantum chemistry calculations, selection of starting points remain critical to the quality of the results obtained. For this preliminary step, an approach based on the interpretative tools of quantum chemistry was chosen: the relative orientation of each partner should be such that interactions between complementary sites are maximized. We have applied this approach to identify both non-covalent complexes and reaction pathways.

All the relative energies mentioned were calculated with respect to all the reagents taken separately, which means  $E(\text{CH}_3\text{COOH}) + E(\text{NH}_2\text{CH}_3) + n E(\text{H}_2\text{O})$ .

In all cases, the energies include the ZPE correction ("Sum of electronic and Zero-Point Energies").

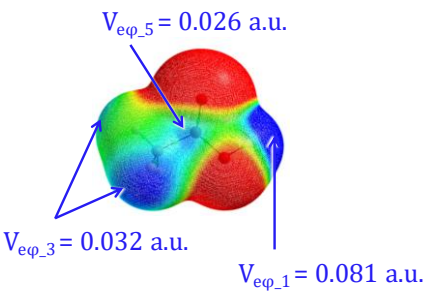
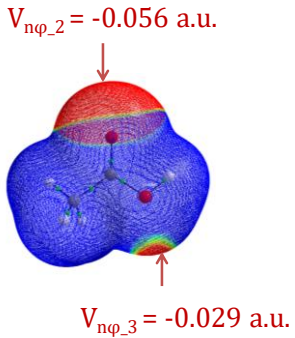
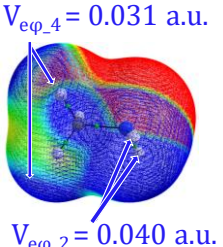
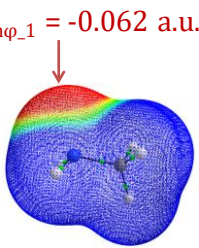
## **Reaction without any water molecules**

### **Caracterization of the isolated reagents**

Based on the assumption that reagents approach each other to maximize interactions between complementary sites, it is natural to study the molecular electrostatic potentials (MESP's) of isolated

reagents to look at their reaction.<sup>35;80-84</sup> However, this approach is quite unusual according to literature, and this is what we are trying to implement in the present work.

The MESP analysis of acetic acid leads to the identification of three electrophilic sites and two nucleophilic sites; the MESP analysis of methylamine leads to the identification of two electrophilic sites and one nucleophilic site (Table 2).

	Electrophilic sites	Nucleophilic sites
Acetic acid <chem>CH3COOH</chem>		
Methylamine <chem>NH2CH3</chem>		

**Table 2: Identification of electrophilic (eφ) and nucleophilic (nφ) sites from the MESP analysis of the acetic acid and the methylamine.**

In order of decreasing electrophilicity, the sites identified are as follows (Figure 1):

- the most electrophilic site, noted eφ<sub>1</sub>, is identified on acetic acid, close to the hydrogen atom of the carboxylic acid function, with a molecular electrostatic potential of 0.081 a.u.,
- the most electrophilic site identified on methylamine, eφ<sub>2</sub>, is located close to the hydrogen atoms of the amine functions, with a molecular electrostatic potential of 0.040 a.u.,
- another electrophilic site, eφ<sub>3</sub>, is identified near the hydrogen atoms of the methyl function of acetic acid, with a molecular electrostatic potential of 0.032 a.u.,
- a fourth electrophilic site, eφ<sub>4</sub>, is identified near the hydrogen atoms of the methyl function of methylamine, with a molecular electrostatic potential of 0.031 a.u.,
- a fifth electrophilic site, eφ<sub>5</sub>, is identified in the vicinity of the sp<sup>2</sup> hybridized carbon atom perpendicular to the plane of the molecule (above and below this plane). Such electrophilic sites are often identified close to chemical unsaturation, especially in the case of C=C and C=O multiple bonds, and are referred to as 'π-holes'.

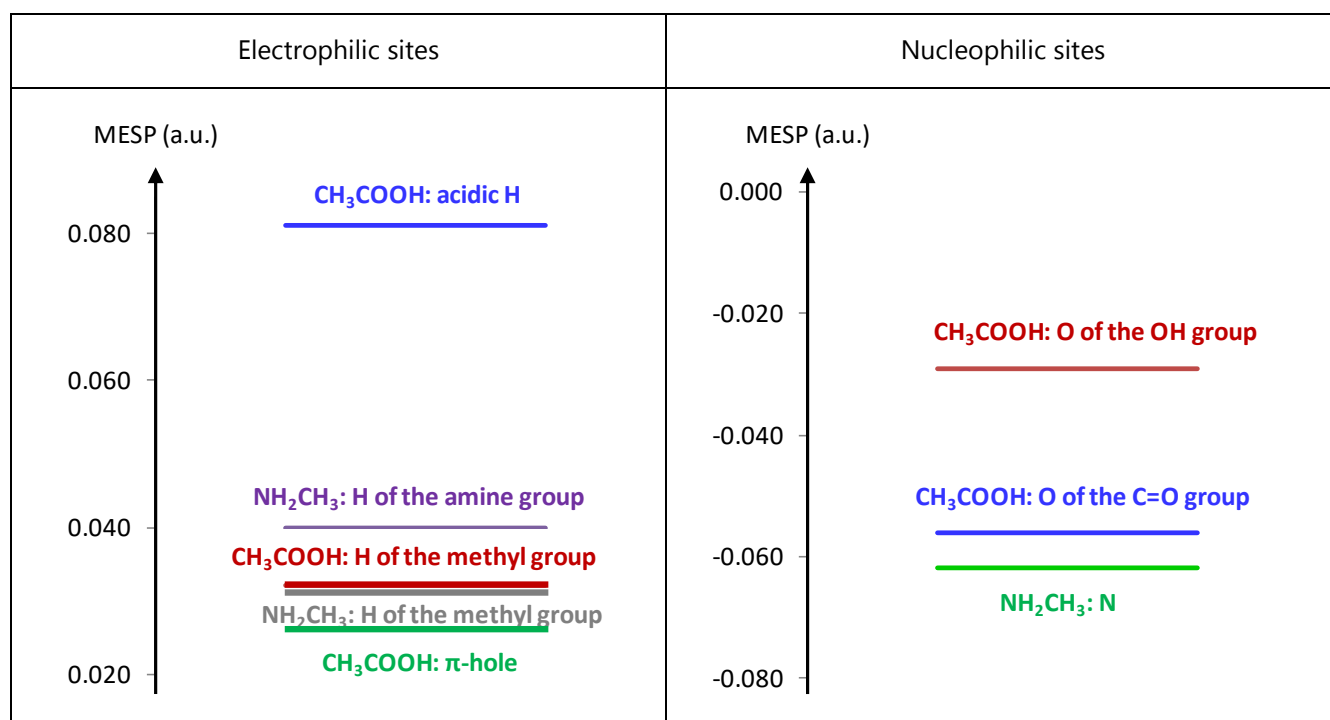


**Figure 1: Classification of the electrophilic and nucleophilic sites available on the reagents.**

In decreasing order of nucleophilicity, the sites identified are as follows:

- the most nucleophilic site, noted  $n\phi_1$ , is identified on methylamine, near the nitrogen atom, with a molecular electrostatic potential of -0.062 a.u.,
- the most nucleophilic site identified on acetic acid, noted  $n\phi_2$ , is located near the oxygen atom of the carbonyl function, with a molecular electrostatic potential of -0.056 a.u.,
- another nucleophilic site, noted  $n\phi_2$ , is identified on the acetic acid, noted  $n\phi_2$ , is located close to the oxygen atom of the OH group, with a molecular electrostatic potential of -0.029 a.u.

Furthermore, for comparative purposes, the  $f^+$  and  $f^-$  Fukui functions as well as the  $f^2$  Dual Descriptor were also calculated for both reagents. As these descriptors are calculated on atoms, the minimum ESP\_MIN and maximum ESP\_MAX atomic values of the electrostatic potential were also determined. [Figure 2](#) shows the values obtained for the C, O and N atoms of the reagents. As in the previous analysis, the nucleophilic character of the nitrogen atom of methylamine is clearly highlighted by these descriptors, with a high  $f^-$  value, a negative  $f^2$  value, and a high ESP\_MIN in absolute value. The nucleophilic character of the oxygen atom of the C=O group of acetic acid is also clearly demonstrated with a high  $f^-$  value, a negative  $f^2$  value, and a high ESP\_MIN in absolute value. In contrast, the  $\pi$ -hole of the carbonyl group of acetic acid is not clearly evidenced by these descriptors. Given its importance in the reaction of interest, these descriptors seem less relevant than the MESP approach presented in Table 2 and [Figure 1](#), in this particular case. This is consistent with the very local and directional aspect of electrostatic interactions involving  $\pi$ -holes. This is why only the MESP approach will be considered in the rest of this study.



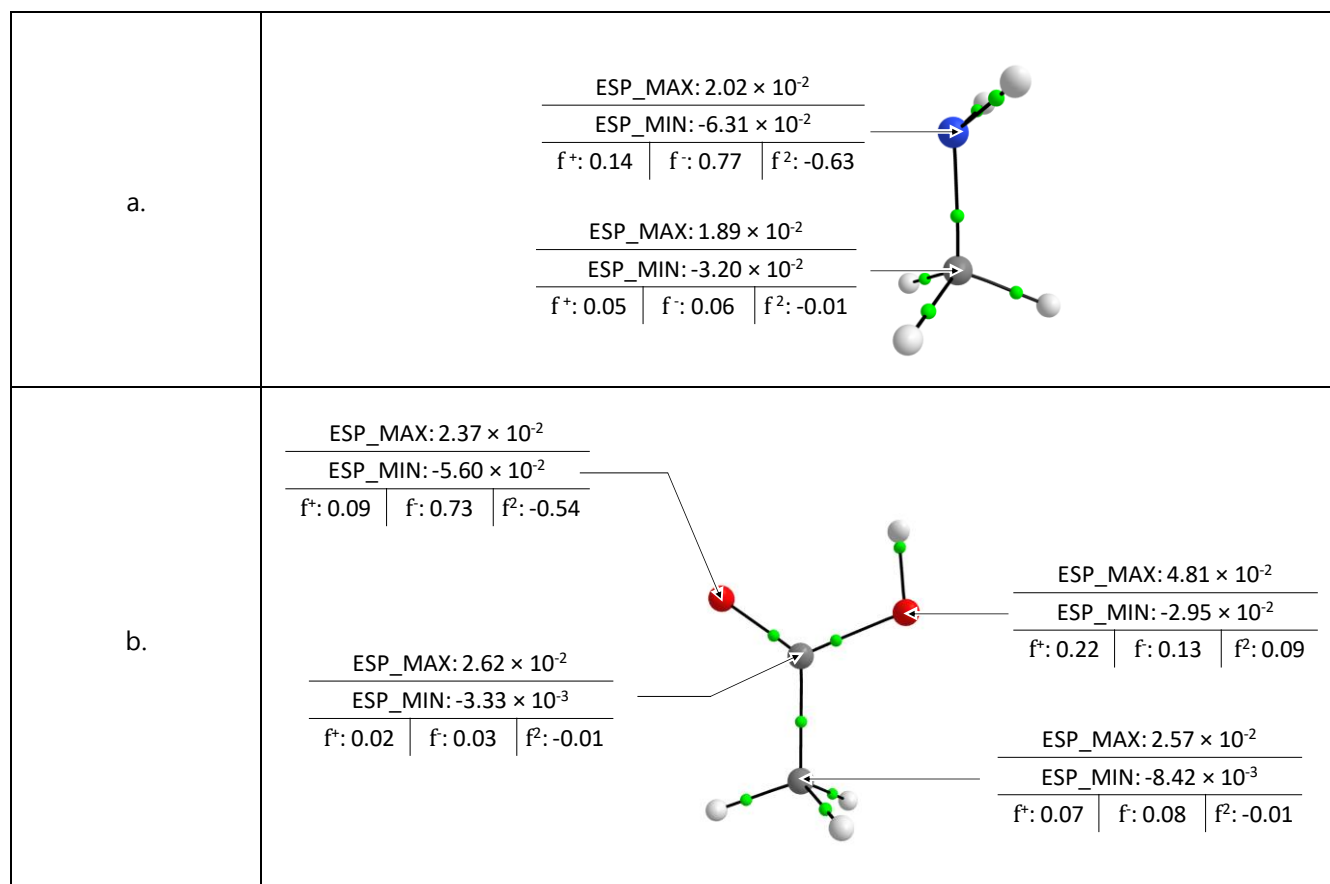


**Figure 2: Values of the minimum ESP\_MIN and maximum ESP\_MAX atomic values of the electrostatic potential, the  $f^+$  and  $f^-$  Fukui functions as well as the  $f^2$  Dual Descriptor for a. methylamine and b. acetic acid.**

In order to further identify non-covalent complexes that may form between acetic acid and methylamine, initial structures are built up such as to maximize interactions between electrophilic sites of one partner and nucleophilic sites of the other partner, following an already reported methodological approach. After geometry optimization, six non-covalent complexes are thus obtained, and are presented in Supporting Information. For the sake of clarity, the complexes were classified in the order of their relative stabilities, and they were named Cplex<sub>1-6</sub>, from the most stable one (Cplex<sub>1</sub>) to the less stable one (Cplex<sub>6</sub>).

The intermolecular interactions in these non-covalent (CH<sub>3</sub>COOH):(NH<sub>2</sub>CH<sub>3</sub>) complexes were investigated in order to search for possible links between the properties of the isolated partners and the complexes formed. This work carries on studies of the Quantitative Structure Activity Relationship (QSAR) type, particularly used in organic chemistry to link the intrinsic properties of isolated molecules to their reactivity. The underlying idea is to search for quantitative descriptors derived from the topological analysis of isolated molecules to help identify non-covalent complexes. In order to do this,, we have plotted for each intermolecular interaction identified in the complexes, the variations of the MESP difference between the electrophilic site and the nucleophilic site of the isolated partners, as a function of the product of the electron density at the BCP point and the internuclear distance, of the interaction formed in the complex (Figure 3).

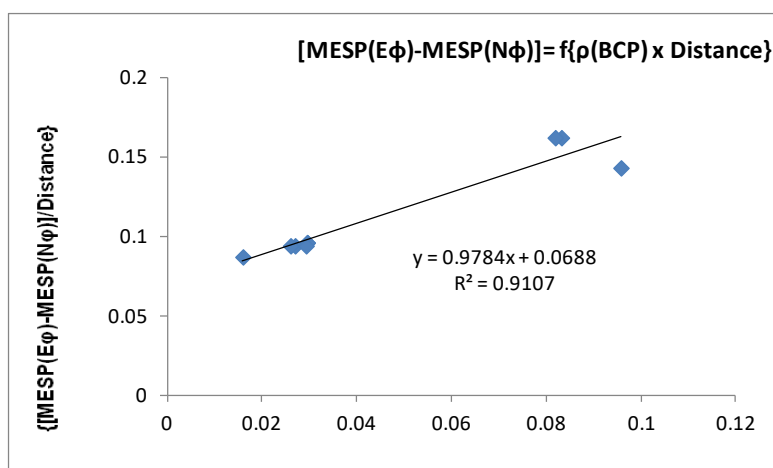


**Figure 3 : Identification of a relationship between the intrinsic properties of the two partners and the complexes (CH<sub>3</sub>COOH)(NH<sub>2</sub>CH<sub>3</sub>) formed. The interaction between the two nucleophilic sites of the Cplex<sub>6</sub> complex was not taken into account.**

**Potential energy surface of the peptide-like bond-forming reaction in the absence of additional water molecules**

Among the non-covalent complexes identified between acetic acid and methylamine, the Cplex<sub>6</sub> complex shown in Figure 4 represents a good candidate as a preliminary step in the formation of the peptide-like bond between acetic acid and methylamine: this complex is obtained by seeking to maximize the interaction between the nucleophilic site located near the nitrogen atom of methylamine and the electrophilic site located near the carbon atom bearing the carboxylic acid function of acetic acid. Although this is not the most stable non-covalent complex between acetic acid and methylamine, the interaction energy associated with the formation of this complex is substantial ( $\Delta E = -14.22$  kJ/mol).

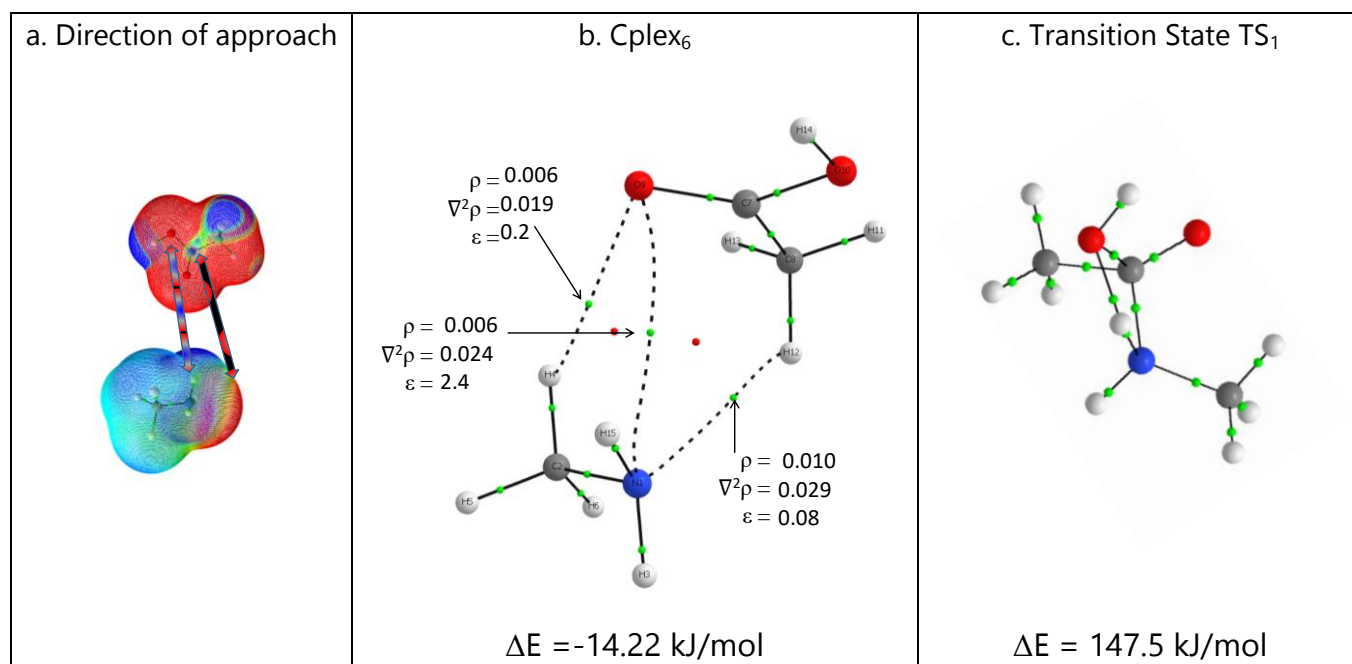


**Figure 4: Identification of the preferential direction of approach of both partners based on the MESP analysis(a), Identification of a non-covalent complex (b) and a transition state (c) for the formation of the peptide-like bond.**

The TS<sub>1</sub> transition state was obtained by considering the same direction of approach as that leading to the identification of the Cplex<sub>6</sub> complex (Table 4). The IRC analysis confirms that the TS<sub>1</sub> and

Cplex<sub>6</sub> structures do indeed constitute two stationary points on the same potential energy surface. Moreover, the IRC analysis also shows that this reaction can occur in a single step (Figure 5), and the energy barrier associated with this reaction is calculated as being 147.5 kJ/mol. This is consistent with literature,<sup>1,3</sup> and shows that this reaction cannot occur spontaneously

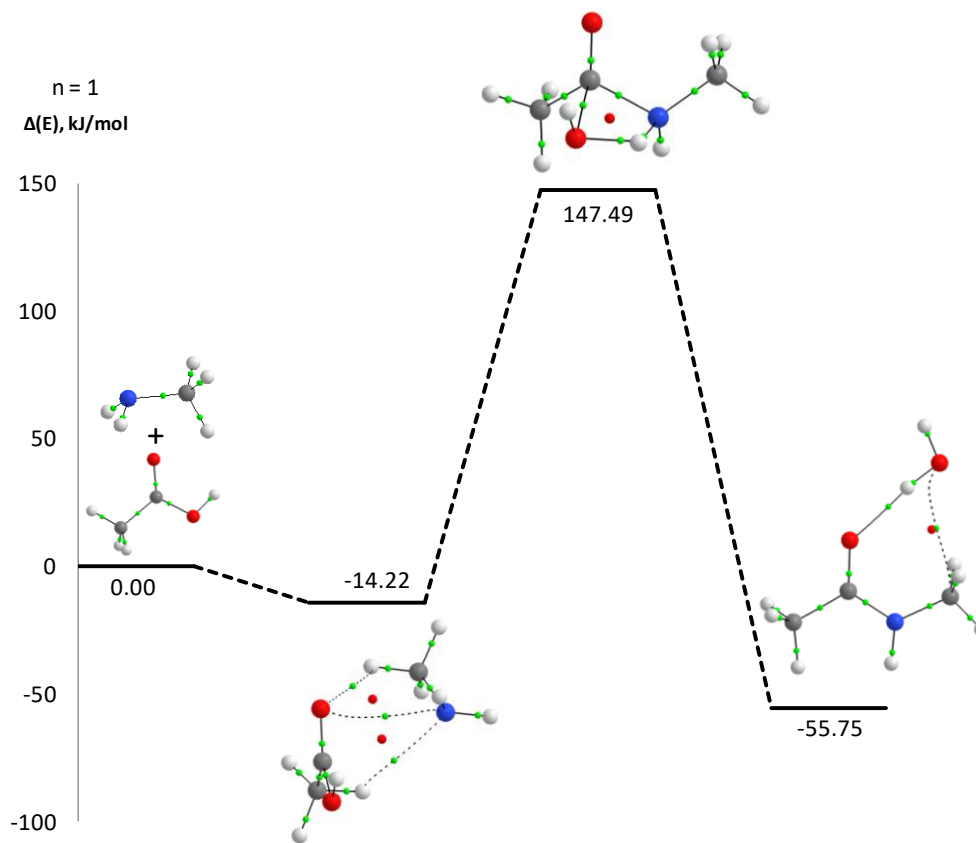


**Figure 5: Energy profile for the peptide-like bond formation reaction between CH<sub>3</sub>COOH and NH<sub>2</sub>CH<sub>3</sub> without any water molecule.**

### Microhydration of the reagents and of the product

The next step was to determine the influence of a small number of water molecules on the reaction profile presented in Figure 5.

In order to do this, the structures of the most stable micro-hydrate complexes for the reagents were identified by applying the same principle of maximizing interactions between complementary sites. This methodology leads to the identification of the same structures as those already reported in literature, by Lv et al.<sup>85</sup> and Krishnakumar et al.,<sup>86</sup> respectively. This verification is relevant. Indeed Krishnakumar studied the microhydration of acetic acid in a very comprehensive way at the calculation levels of  $\omega$ B97XD/aug-cc-pVDZ and CCSD(T)/6-311++G(d,p). Lv used the BH algorithm, combining the Metropolis sampling technique and local optimizations to identify the global minima on the potential energy surfaces of complexes (NH<sub>2</sub>CH<sub>3</sub>)(H<sub>2</sub>O)<sub>1-7</sub>, at the PW91/6-311++G(3df,3pd) computation level. Their studies can thus be used as references. The fact that the global minima predicted by the approach used here are the same as those reported in the literature makes it possible to validate the use of MESP analysis and the definition of preferred directions of approaches by maximizing interactions between complementary sites. All the Cartesian Coordinates are presented in Supplementary Information.

Additionally, the most stable structures for microhydrated dimethylacetamide complexes were also investigated. One of the most recent reference studies on the topic was done by Kang et al.<sup>87</sup> In this study, microhydrated complexes involving between 1 and 3 molecules of water were studied in CCSD(T), MP2 and DFT.

Our methodology leads to the identification of the same most stable complexes. An almost iso-energetic structure ( $\Delta E = 0.5$  kJ/mol) is obtained for the dihydrated complex. This structure and those of complexes involving more water molecules are presented in Supplementary Information.

### **Reaction pathways win the presence of one to five water molecules**

With regard to the methodology used, which consists in maximizing interactions between complementary sites of the partners, one of the difficulties in this case is to make a relevant choice of partners. We focused on two strategies: the study of the microhydration of the transition state identified in the case of the reaction without a water molecule, and the study of the microhydration of the reagents before the formation of a pre-reagent complex. Why does both approaches appear to be particularly relevant?

- First of all, the study of the microhydration of the transition state should lead, a priori, to the reaction paths associated with the lowest energy barriers. Indeed, the MESP analysis of the transition state of the reaction pathway without water molecule will allow to identify the most electrophilic and nucleophilic sites, and their optimal interaction with water molecules should lead, a priori, to a decrease of the energy barrier. It Therefore , it seems essential to determine whether reaction pathways that could involve these "stabilized transition states" could exist, and if so, to identify them.
- Alternatively, the study of the microhydration of reagents also seems unavoidable within the framework of the search for reaction paths in the presence of water molecules. Indeed, from a mechanistic point of view, the water molecules could form complexes with the reagents, which could be more stable than those that could be identified by the first approach.

Thus, the study of the microhydration of the transition state identified without a water molecule could lead to the identification of the reaction pathways associated with the lowest energy barrier compared to all the reagents taken in isolation. Alternatively, the study of the microhydration of the isolated reagents should lead to the identification of the reaction pathways involving the most stable pre-reagent complexes. It should be noted that the study of the microhydration of the pre-reagent complex identified without water molecule leads to the identification of the same reaction pathways.

The results obtained using these different strategies will be presented and analyzed, before being outlined with respect to previous studies reported in literature.

To keep the discussion as clear as possible, the structures discussed will be named according to the approach used, and according to their relative stability:

- in the case of structures identified from the microhydration of TS, the most stable TS obtained in the presence of  $n$  water molecules will be referred to as  $TS_1^{Wn-A}$ . For each most stable TS identified for a given number of water molecules, the complete reaction path has

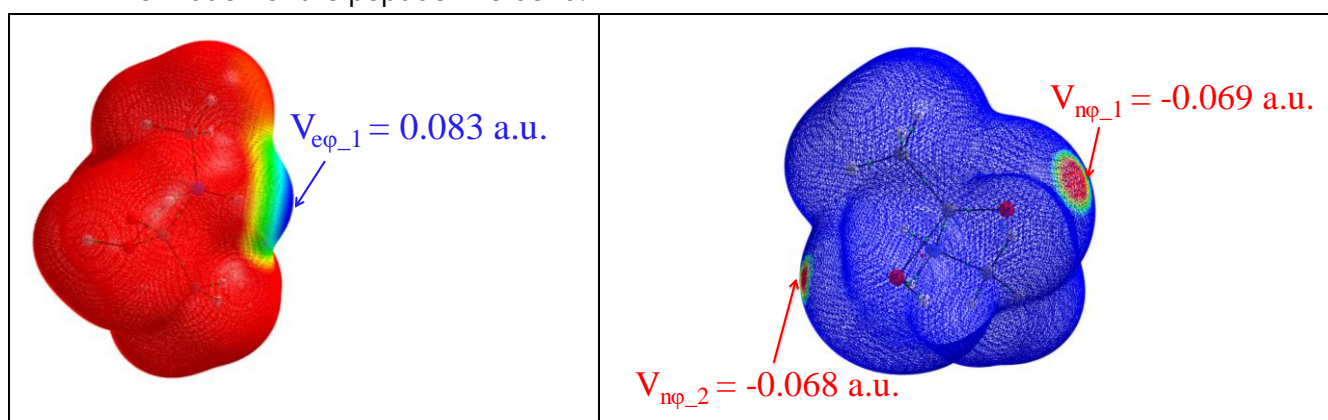
been investigated. The pre-reactive complex and the final state corresponding to  $TS_1^{Wn-A}$  will be referred to as  $Cplex_1^{Wn-A}$  and  $Final_1^{Wn-A}$ , respectively,

- in the case of structures identified from the microhydration of the reagents, the most stable  $(CH_3COOH)(NH_2CH_3)(H_2O)_n$  complex identified as a first step in the reaction of the peptide-like bond formation in the presence of  $n$  water molecules will be referred to as  $Cplex_1^{Wn-B}$ . For each of the  $Cplex_1^{Wn-B}$  identified for a given  $n$  number of water molecules, the complete reaction path was investigated. The TS and the final state corresponding to the  $Cplex_1^{Wn-B}$ , will be named  $TS_1^{Wn-B}$  and  $Final_1^{Wn-B}$ , respectively.

### Microhydration of the transition state

Let's assume two hypotheses:

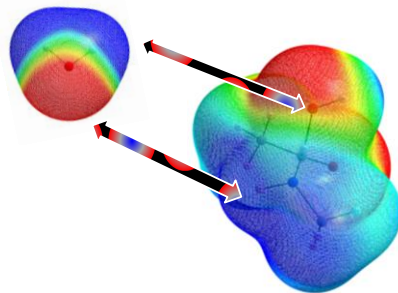
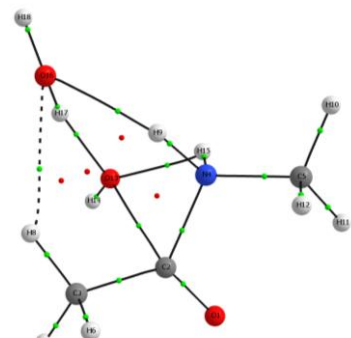
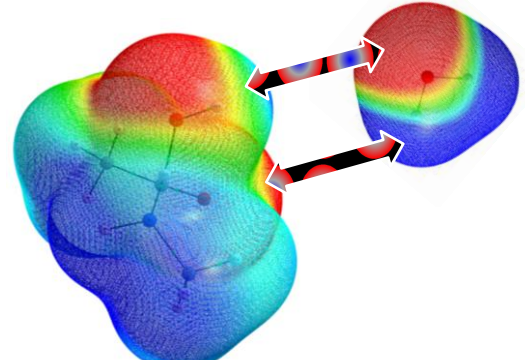
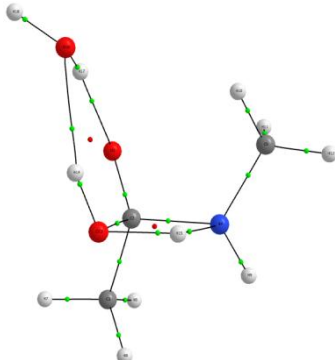
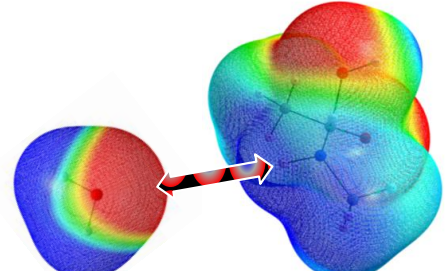
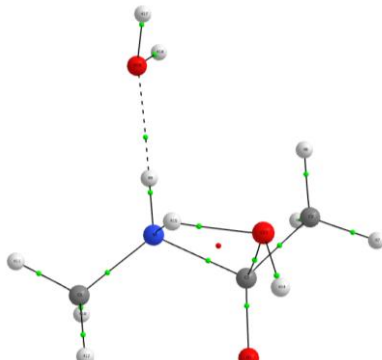
- the presence of a few water molecules facilitates the reaction to form the peptide-like bond,
- microhydration does not dramatically alter the reaction pathway associated with the formation of the peptide-like bond.



**Figure 6: Identification of an electrophilic site and two nucleophilic sites on the non-hydrated transition state  $TS_1$ .**

Within the framework of these two hypotheses, it is relevant to characterize the MESP of the transition state of the reaction without water molecule, and to identify the preferred approach directions of water molecules to best interact with the available electrophilic and nucleophilic sites. The MESP analysis of the transition state ([Figure 6](#)) leads to the identification of three significant sites of interaction.

An electrophilic site is identified near the hydrogen atom of the amine function which is not impacted by the reaction. Two nucleophilic sites are identified near each of the oxygen atoms. From this analysis, different directions of approach can be identified, as shown in [Table 3](#) in the case of a single water molecule interacting with  $TS_1$ .

Considered direction of approach on the basis on the MESP analysis	Structures and energies of the optimized microhydrated transition states
	 <p><math>\Delta E = 96.93 \text{ kJ/mol. TS}_1^{\text{W1-A}}</math></p>
	 <p><math>\Delta E = 110.04 \text{ kJ/mol. TS}_2^{\text{W1-A}}</math></p>
	 <p><math>\Delta E = 122.34 \text{ kJ/mol. TS}_3^{\text{W1-A}}</math></p>

**Table 3: Microhydration of  $\text{TS}_1$  with one water molecule: Identification of possible directions of approaches from the MESP, and structures and energies of the optimized microhydrated transition states.**

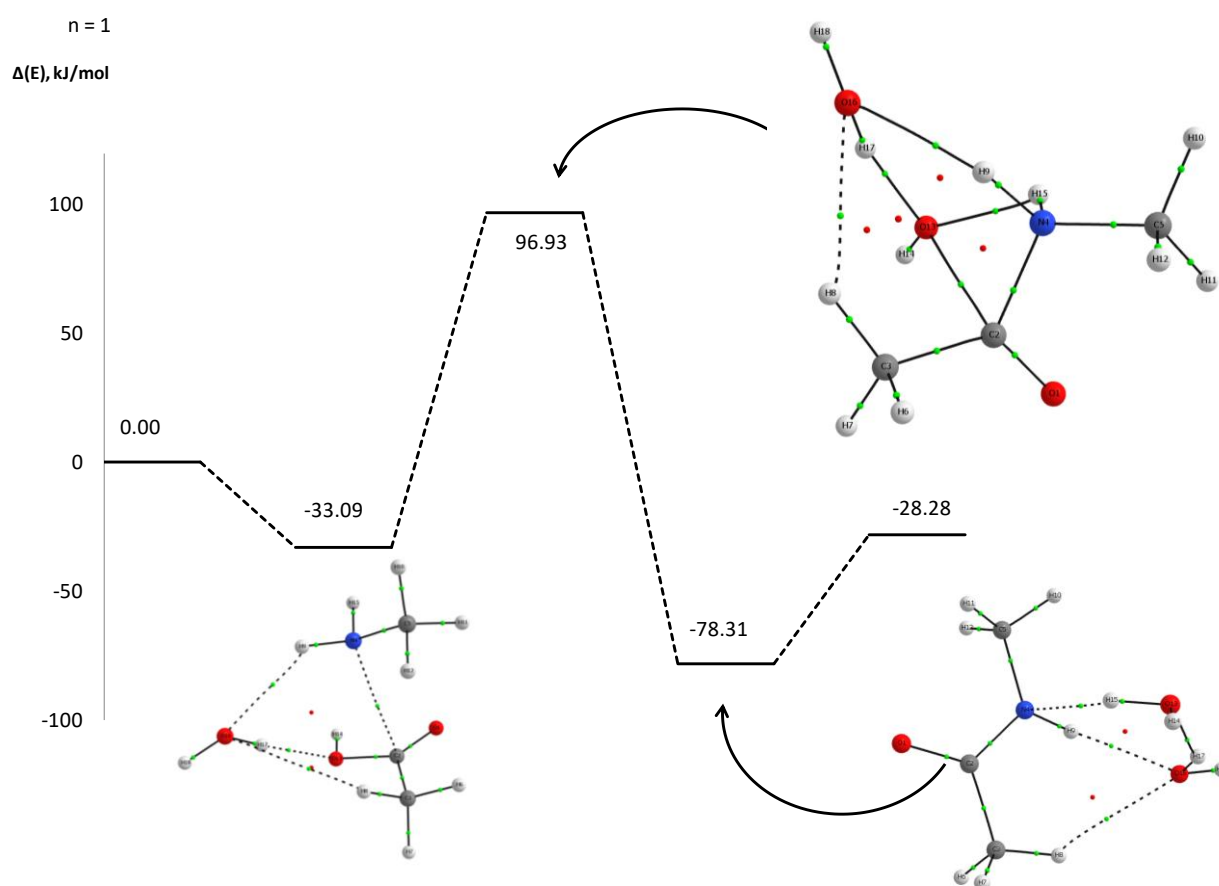
In the first structure obtained by order of stability,  $\text{TS}_1^{\text{W1-A}}$ , the water molecule acts both as a hydrogen bond donor with respect to the oxygen atom leading to the loss of the water molecule, and as a hydrogen bond acceptor with respect to the hydrogen atom of the amine function which is not a priori directly involved in the reaction. This is the most stable structure obtained for the transition state; this structure is located 96.93 kJ/mol above the separated partners.

In the second structure obtained in order of stability,  $\text{TS}_2^{\text{W1-A}}$ , the water molecule acts both as a hydrogen bond donor with respect to the oxygen atom of the C=O group and as a hydrogen bond

acceptor with respect to the alcohol function of the acetic acid. This structure is located 110.04 kJ/mol above the separated partners.

In the third structure obtained in order of stability,  $TS_3^{W1-A}$ , the water molecule interacts as a hydrogen bond acceptor with the hydrogen atom of the amine function which is not directly involved in the reaction. This structure is located 122.34 kJ/mol above the separated partners.

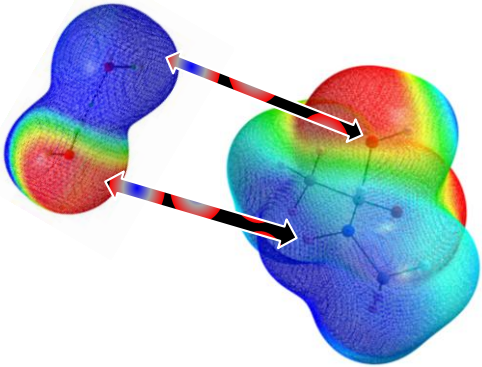
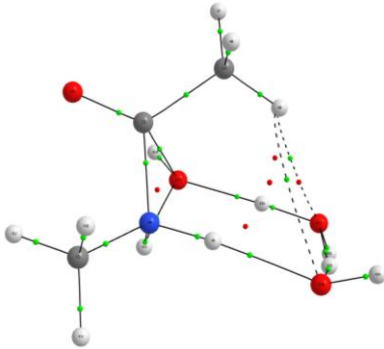
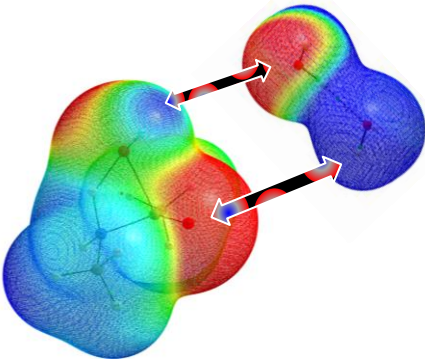
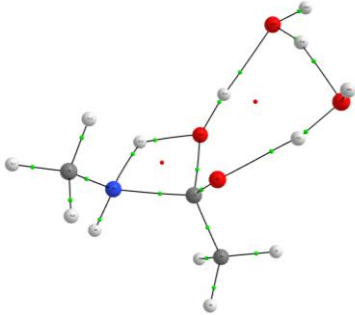
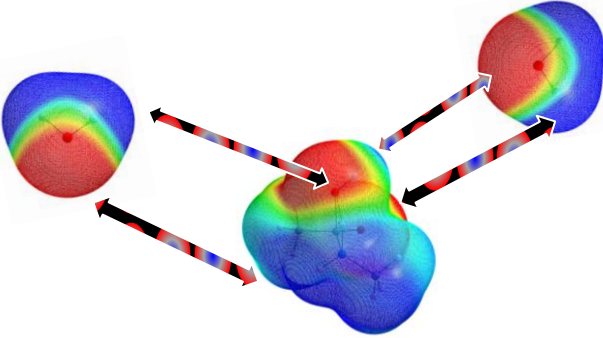
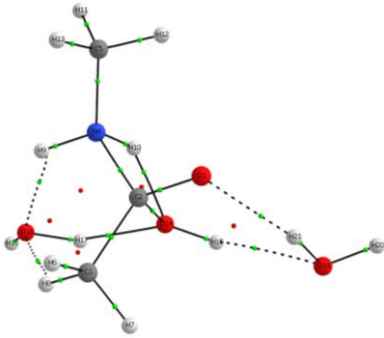
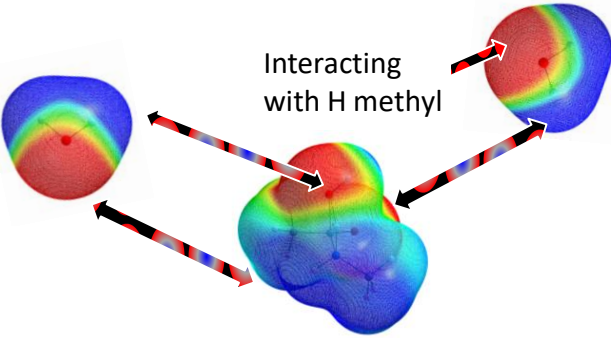
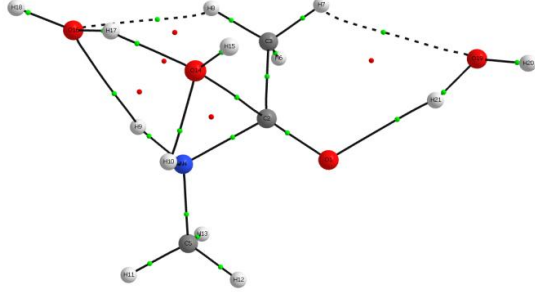
Finally, the most favourable reaction path with a water molecule of hydration leads to the transition state in which the water molecule interacts simultaneously as a hydrogen bond donor with the OH group of the acetic acid, and as a hydrogen bond acceptor with the amine function ( $TS_1^{W1-A}$ ). This reaction leads to the formation of water dimer interacting with the dimethylacetamide (Figure 7).



**Figure 7: Energy profile for the peptide-like bond formation reaction involving the most stable monohydrated transition state identified.**

Two preferential directions of approaches are identified from the MESP analysis from the dimer to the transition state (Table 4).



Considered direction of approach on the basis on the MESP analysis	Structures and energies of the optimized microhydrated transition states
	 <p><math>\Delta E = 36.14 \text{ kJ/mol. TS}_1^{\text{W2-A}}</math></p>
	 <p><math>\Delta E = 70.02 \text{ kJ/mol. TS}_2^{\text{W2-A}}</math></p>
	 <p><math>\Delta E = 73.73 \text{ kJ/mol. TS}_3^{\text{W2-A}}</math></p>
 <p>Interacting with H methyl</p>	 <p><math>\Delta E = 74.88 \text{ kJ/mol. TS}_4^{\text{W2-A}}</math></p>

**Table 4: Microhydration of  $\text{TS}_1$  with two water molecules: Identification of possible directions of approaches from the MESP, and structures and energies ( $\Delta E$ , in kJ/mol) of the optimized microhydrated transition states.**



In the most stable isomer,  $TS_1^{W2-A}$ , the water dimer interacts as a hydrogen bond donor to the OH group of the acetic acid. At the same time, the water dimer interacts as a hydrogen bond acceptor with respect to the hydrogen atom of the amine function which is not a priori directly involved in the reaction. This transition state is 36.14 kJ/mol above the isolated partners (i.e. two isolated water molecules, the acetic acid and the methylamine).

A second structure,  $TS_2^{W2-A}$ , corresponds to the water dimer interacting with the carboxylic acid group: the water dimer simultaneously acts as a hydrogen bond donor with respect to the C=O group and as a hydrogen bond acceptor with respect to the OH group of the acetic acid. This structure is 70.02 kJ/mol above the isolated partners, which means that it is much less favorable than the  $TS_1^{W2-A}$  transition state.

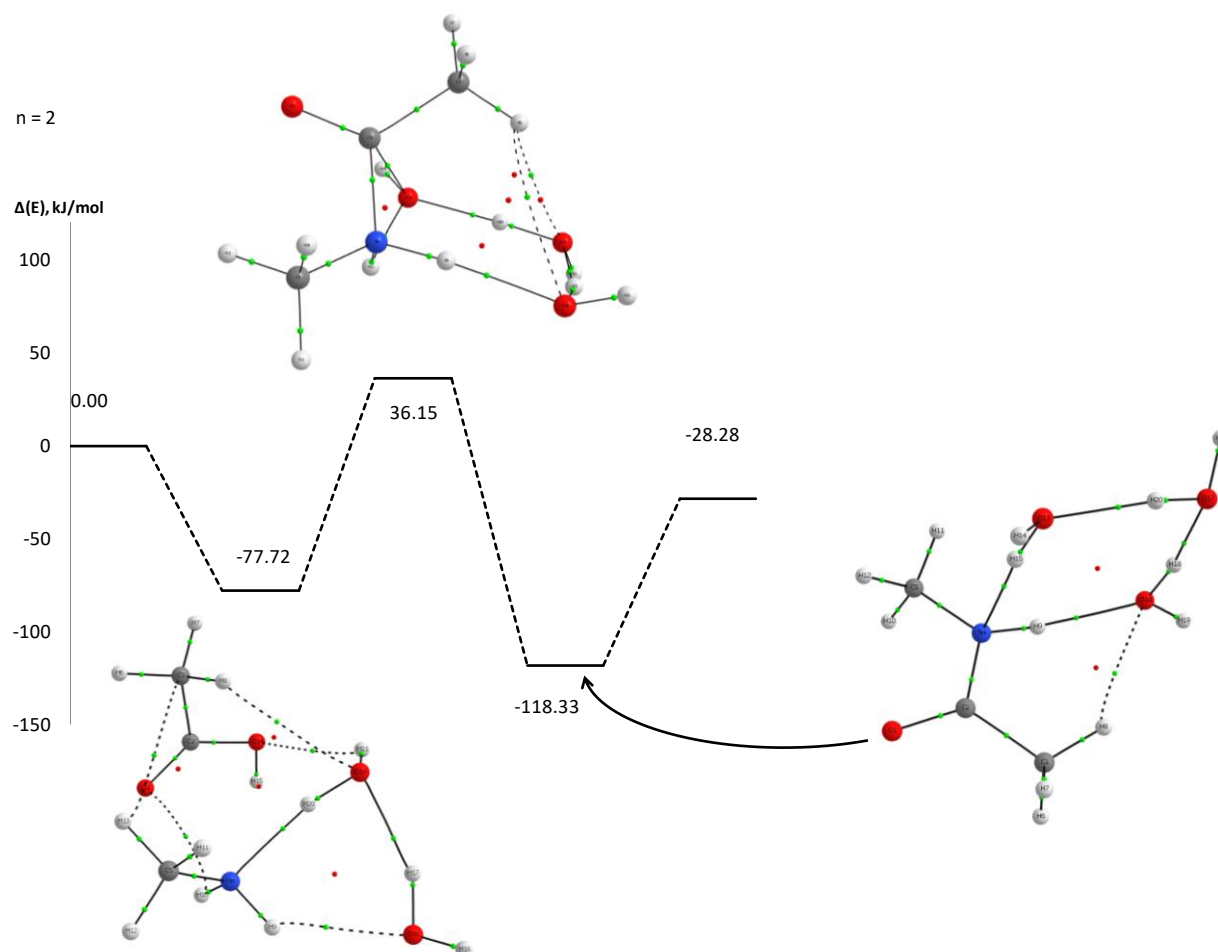
In the case of the reaction occurring with two water molecules, it is of course necessary to compare the energies of the structures obtained when considering a dimer interacting with the TS, with the energies of the structures obtained when considering two water molecules interacting separately with the TS. It has indeed been previously reported that :

- in the case of apolar solutes, the interaction of water clusters is often energetically more favourable than the interaction of isolated water molecules. A term has been introduced to name this privileged interaction of water clusters with a solute: "segregation of water molecules",<sup>36,88,89</sup>
- on the contrary, in the presence of polar solutes, it has been shown in some cases that the interaction of isolated water molecules could be energetically more favourable than the interaction of a unique water cluster.<sup>90</sup>

Thus, for the reaction involving  $n$  water molecules, the interactions of  $(H_2O)_n$  clusters,  $n$  isolated water molecules and all combinations of small  $(H_2O)_x$  and  $(H_2O)_y$  aggregates such that  $x+y=n$ , were studied.<sup>91</sup>

In the case of the TS interacting with two water molecules, we sought to identify the preferred directions of approaches of two separate water molecules. In this case, one of the water molecules can interact simultaneously with one of the hydrogen atoms of the methyl group and with the oxygen atom of the OH group, in a similar way to what has been found in the  $TS_1^{W1-A}$ . The second water molecule can interact with the oxygen atom of the carbonyl group, and either with one of the hydrogen atoms of the methyl group or with the hydrogen atom of the OH group. The structures obtained after geometry optimization for both these cases are located 73.73 and 74.88 kJ/mol above the isolated partners, respectively. These structures in which both water molecules interact separately with the TS are thus energetically much less favorable than the  $TS_1^{W2-A}$  transition state (Table 4).

Finally, with only two molecules of water present in the gas phase, the energy barrier associated with the formation of methylacetamide from methylamine and acetic acid is lowered by about 110 kJ/mol, from 147.49 kJ/mol to 36.15 kJ/mol (Figure 8). The product formed consists of a dimethylacetamide molecule interacting with three molecules of water. These three water molecules correspond to an open form of the water trimer: one of the water molecules acts as a hydrogen bond donor to the nitrogen atom, another water molecule acts as a hydrogen bond acceptor to the hydrogen atom of the acetamide function, and the third water molecule interacts with the other two water molecules.

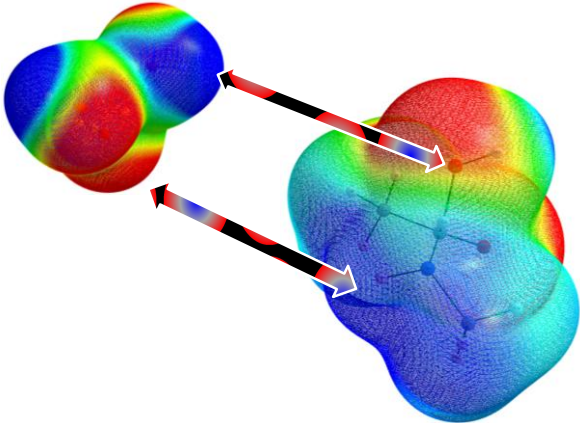
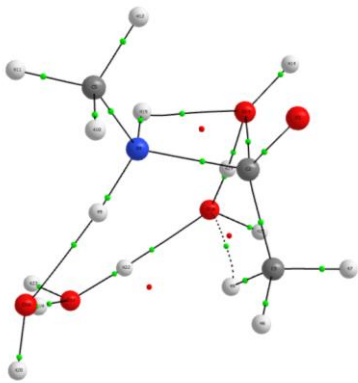
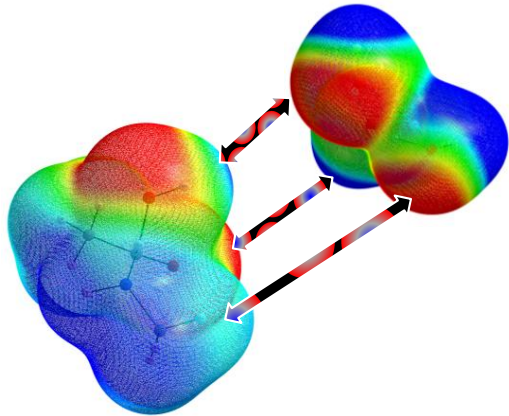
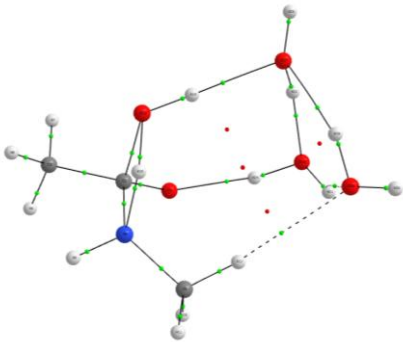
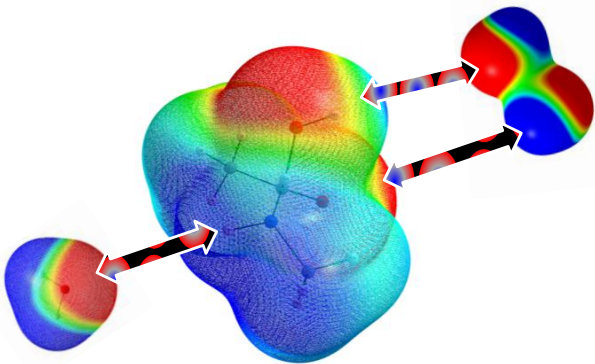
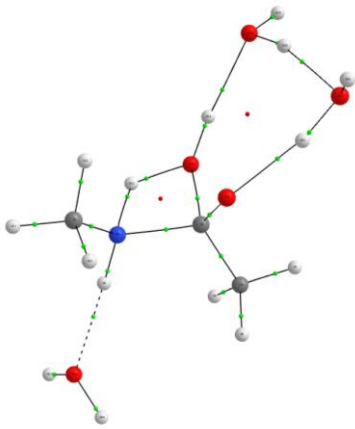


**Figure 8: Energy profile for the peptide-like bond formation reaction involving the most stable dihydrated transition state identified.**

The directions of approach of three water molecules toward  $TS_1$  and leading to the most stable structures are shown in [Table 5](#). The interaction of a water trimer simultaneously with the most electrophilic site and one of the most nucleophilic sites of the solute leads to the most stable structure:  $TS_1^{W3\_A}$ . As has been observed with other solutes, the cyclic structure of the water trimer opens during the optimization, so that only the water molecule that does not interact with the solute forms hydrogen bonds with the other two water molecules. One of the water molecules acts as a hydrogen bond donor to the OH group of the solute, and the other water molecule interacts as a hydrogen bond acceptor to the hydrogen atom of the amine function which is not a priori directly involved in the reaction. This structure is located 5.64 kJ/mol below the separated partners, which means that no energy barrier would be associated with its formation.

The approach of the water trimer on the other side of the solute leads to the  $TS_2^{W3\_A}$  structure. In this structure, the cyclic form of the water trimer is conserved, and the water trimer interacts both as a hydrogen bond donor with the C=O function of the solute, as a hydrogen bond acceptor with the O-H function of the solute, and with one of the methyl groups. This structure is significantly less energy favorable than the previous one, and is 44.75 kJ/mol above the separated partners.

Alternatively, the  $TS_3^{W3\_A}$  structure corresponds to the separate interaction of a dimer and a water molecule. Four hydrogen bond type interactions are identified in the resulting structure: one interaction with the nitrogen atom of the amine function, two interactions with the carboxylic acid group, and a hydrogen bond between the two water molecules. Finally, this structure is located 48.47 kJ/mol above the isolated partners.

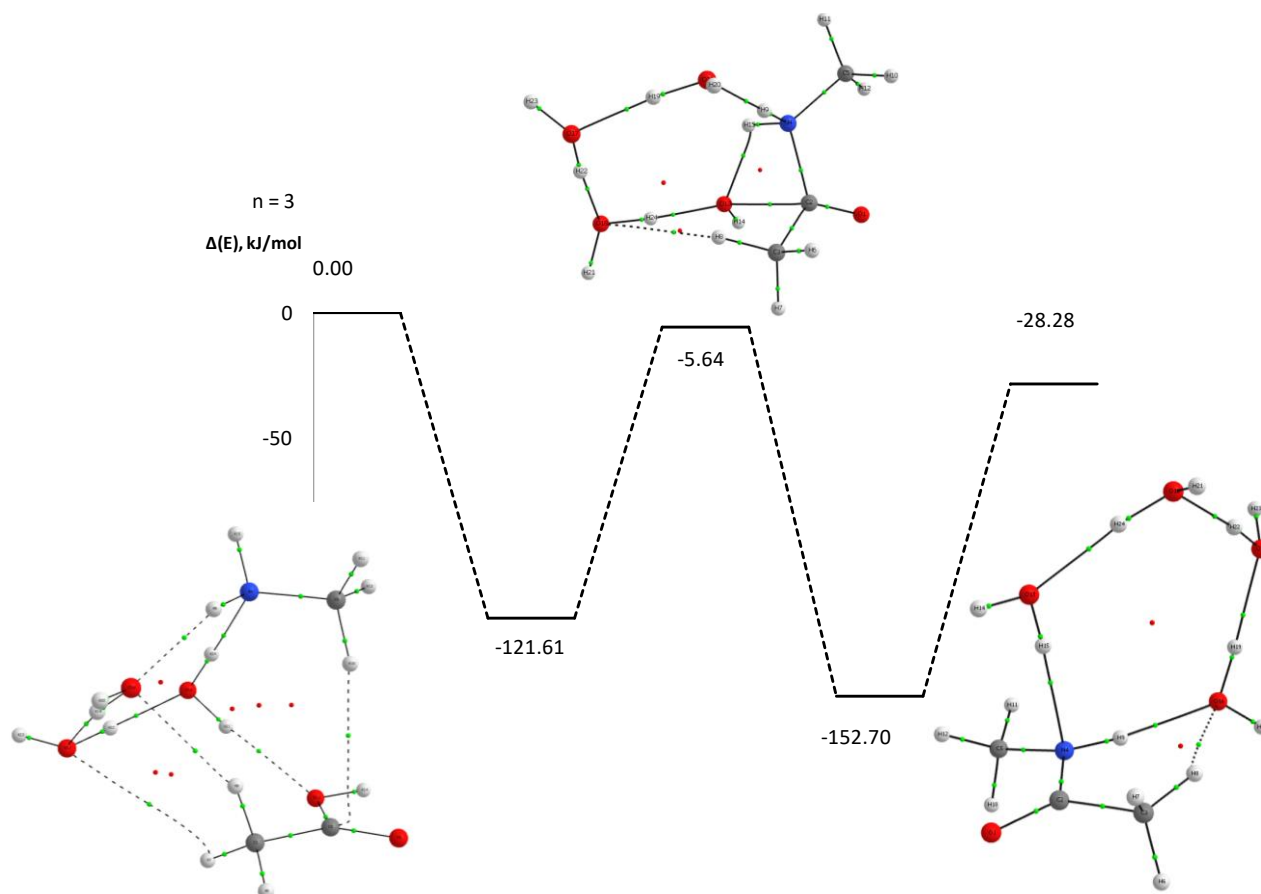
Considered direction of approach on the basis on the MESP analysis	Structures and energies of the optimized microhydrated transition states
	 $\Delta E = -5.64 \text{ kJ/mol. TS}_1^{\text{W3\_A}}$
	 $\Delta E = 44.75 \text{ kJ/mol. TS}_2^{\text{W3\_A}}$
	 $\Delta E = 48.47 \text{ kJ/mol. TS}_3^{\text{W3\_A}}$

**Table 5: Microhydration of  $\text{TS}_1$  with three water molecules: Identification of possible directions of approaches from the MESP, and structures and energies of the optimized microhydrated transition states.**

The most energetically favorable reaction pathway thus identified involves the formation of a non-covalent complex in which an opened form of water trimer interacts simultaneously with methylamine and acetic acid. This complex is located 121.61 below the separated partners.

The transition state can be understood as the formation of a hydrogen bond bridge between the hydrogen atom which is a priori not directly involved in the reaction, from the amine function to the oxygen atom of the OH group of the acetic acid. This TS leads to the formation of

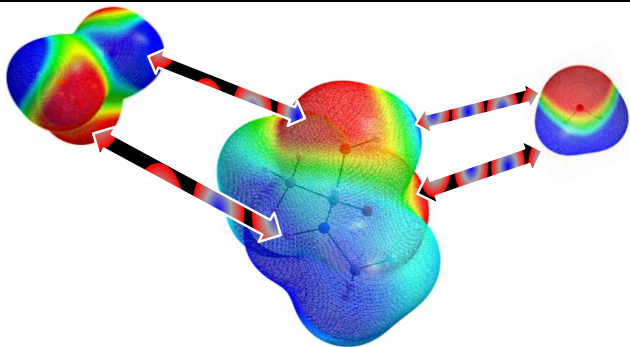
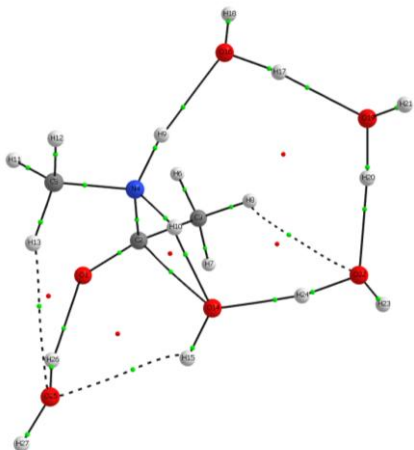
dimethylacetamine, in interaction with a chain of four water molecules linked together by a network of hydrogen bonds (Figure 9).

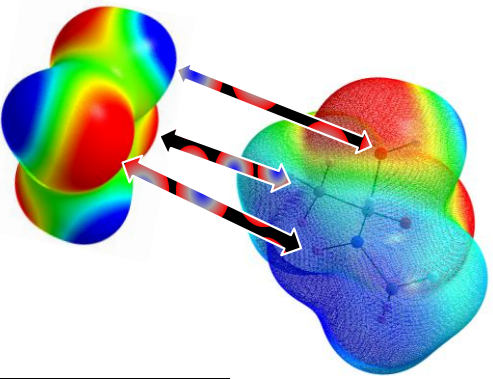
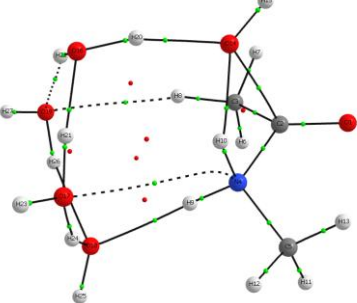
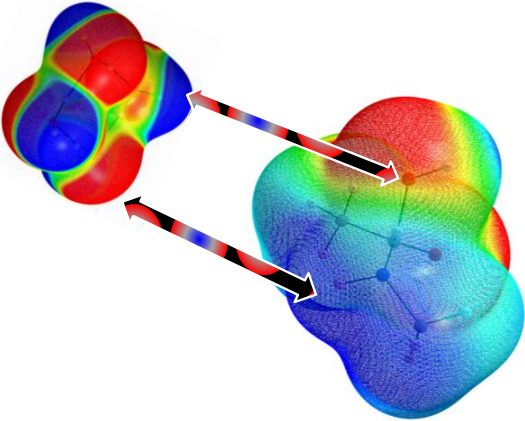
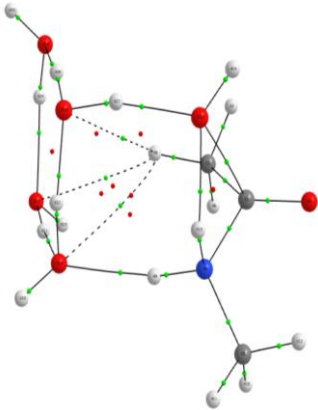
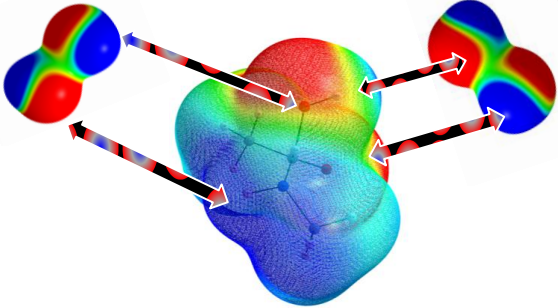
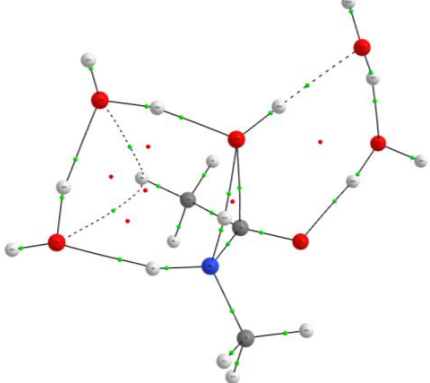
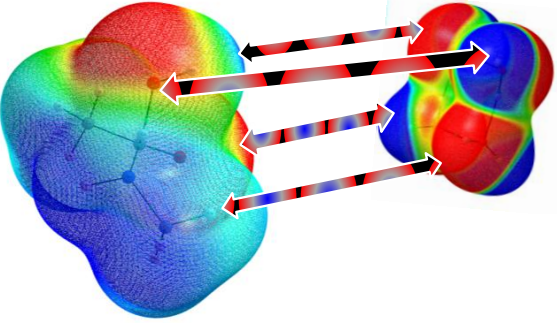
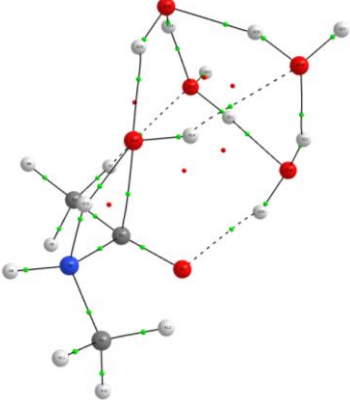


**Figure 9: Energy profile for the peptide-like bond formation reaction involving the most stable transition state identified with three water molecules ( $TS_1^{W3\_A}$ ).**

The directions of approach of four water molecules toward  $TS_1$  and leading to the most stable structures are shown in Table 6.

The most stable water tetramer consists of a cyclic structure characterized by alternating electrophilic and nucleophilic sites. On the other hand, the solute is characterized by an electrophilic site and a nucleophilic site located on either side of the C-N bond which is formed during the reaction.

Considered direction of approach on the basis on the MESP analysis	Structures and energies of the optimized microhydrated transition states
	

	<p><math>\Delta E = -31.74 \text{ kJ/mol. TS}_1^{W4\_A}</math></p>  <p><math>\Delta E = -23.75 \text{ kJ/mol. TS}_2^{W4\_A}</math></p>
	 <p><math>\Delta E = -21.36 \text{ kJ/mol. TS}_3^{W4\_A}</math></p>
	 <p><math>\Delta E = -20.78 \text{ kJ/mol. TS}_4^{W4\_A}</math></p>
	 <p><math>\Delta E = -3.42 \text{ kJ/mol. TS}_5^{W4\_A}</math></p>

**Table 6: Microhydration of TS<sub>1</sub> with four water molecules: Identification of possible directions of approaches from the MESP, and structures and energies of the optimized microhydrated transition states.**

Therefore, it seems particularly relevant in this case to focus on the interaction of smaller clusters of water with the solute. Thus, the most stable TS,  $TS_1^{W4\_A}$ , is obtained by the simultaneous interaction:

- of the water trimer in the same way that led to the structure of the most stable trihydrated TS,
- and of an isolated water molecule on the carboxylic acid group side.

This transition state is 31.74 kJ/mol below the six isolated partners (i.e both reagents, and the four water molecules taken separately). The corresponding reaction path is shown in [Figure 10](#).

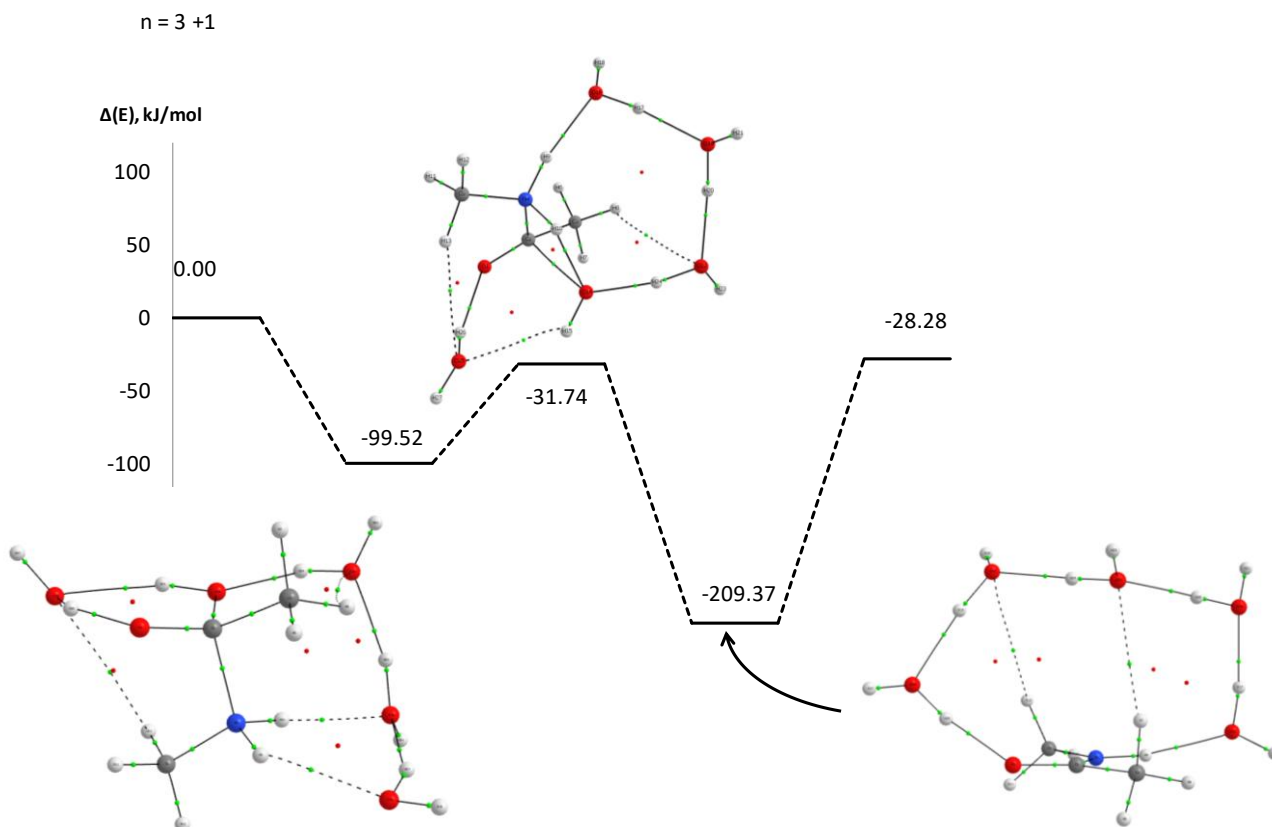


**Figure 10: Energy profile for the peptide-like bond formation reaction involving the most stable transition state identified with four water molecules for the C-N bond formation reaction,  $TS_1^{W4\_A}$ .**

The interaction of the water tetramer with the most electrophilic site and one of the most nucleophilic sites of the solute leads to the identification of the  $TS_1^{W4\_A}$  structure: one of the water molecules acts as a hydrogen bond donor with the OH group and another water molecule acts as a hydrogen bond acceptor with the NH group. Secondary interactions are also identified with one of the methyl groups. One of the water molecules does not interact at all with the solute. This TS is located 23.75 kJ/mol below the isolated partners, and the corresponding reaction path is shown in [Figure 11](#).



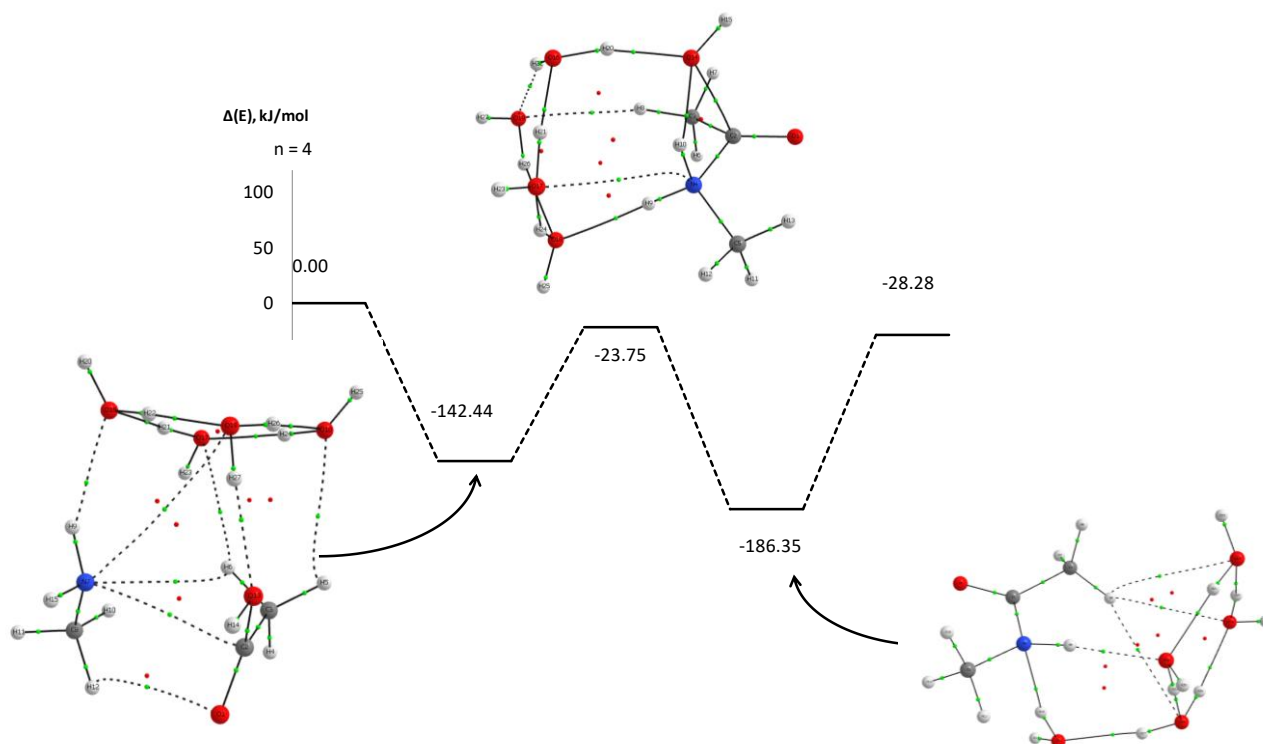


**Figure 11: Energy profile for the peptide-like bond formation reaction involving involving an alternative  $TS_2^{W4\_A}$  transition state in which the water tetramer interact with  $TS_1$ .**

Thus the TS associated with this reaction mechanism is energetically less stable than the one identified with the  $TS_1^{W4\_A}$  structure. However, it is interesting to note that both reaction mechanisms occur without any energy barrier with respect to the different partners taken separately. Furthermore, the formation of the pre-reactant complex is energetically more favourable in the case of the tetramer interacting with the reagents, compared to the separate interaction with a water trimer and a water molecule ([Figure 10](#)).

Another structure similar to  $TS_2^{W4\_A}$  with the water tetramer interacting with the methyl group, the OH group and the amine group is located 21.36 kJ/mol below the isolated partners ( $TS_3^{W4\_A}$ ). The structure in which the tetramer interacts exclusively with the carboxylic acid function of the solute is energetically less favorable ( $TS_5^{W4\_A}$ ): it lies 3.42 kJ/mol below the separate partners.

The transition state involving the simultaneous interaction of two separate water dimers with the solute is calculated as being quasi-isoenergetic with the  $TS_2^{W4\_A}$  structure: this is the  $TS_4^{W4\_A}$  structure, calculated as being 20.78 kJ/mol below the partners taken separately. The reaction path identified from this TS is shown in [Figure 12](#): it involves the formation of a complex consisting of two water dimers interacting simultaneously with the two partners. The stabilization energy associated with the formation of this complex is -113.62 kJ/mol. The product obtained consists of a chain of five water molecules interacting with the dimethylacetamide.

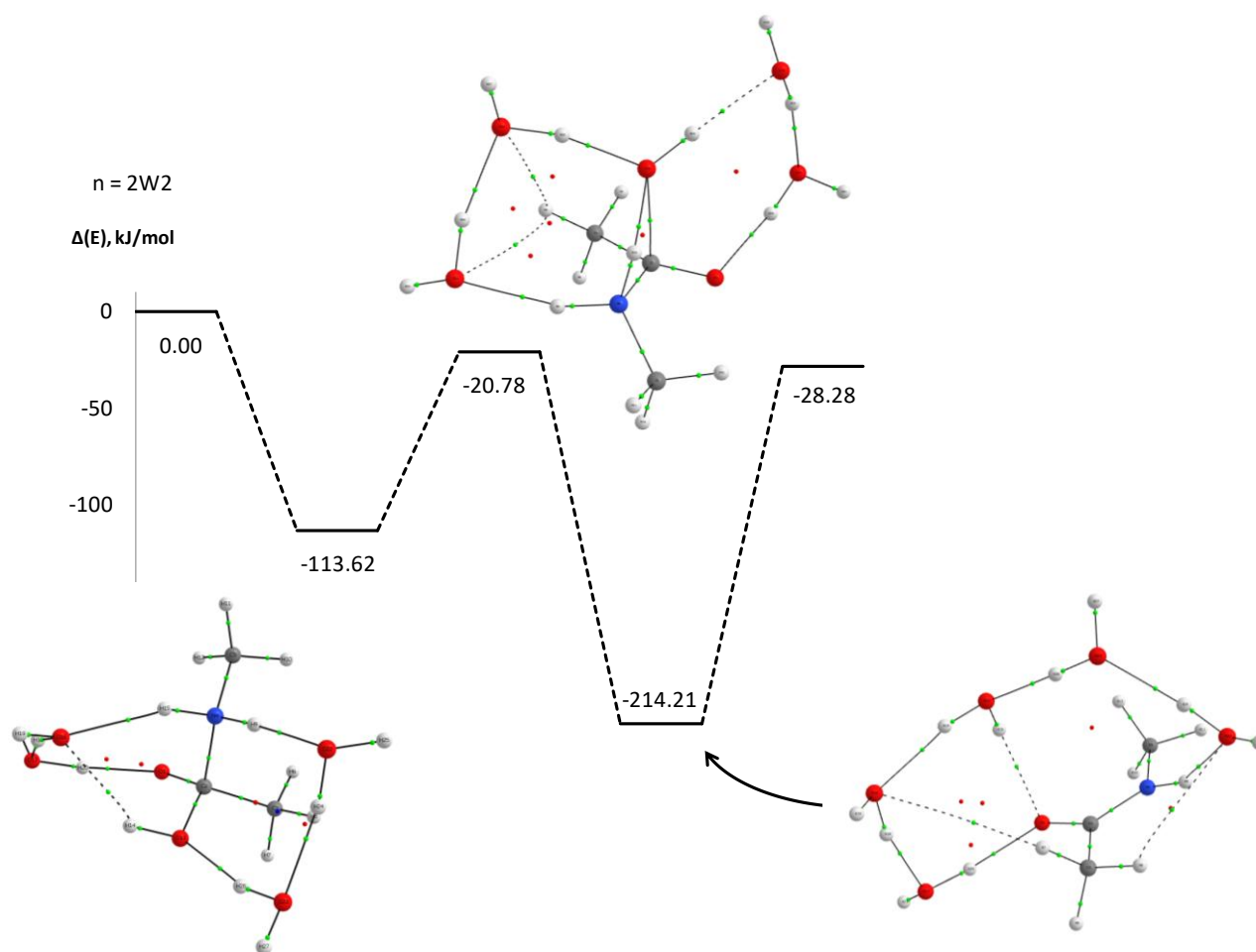


**Figure 12: Energy profile for the peptide-like bond formation reaction involving an alternative  $TS_4^{W4,A}$  transition state in which two separate water dimer interact with  $TS_1$ .**

The directions of approach of five water molecules towards  $TS_1$  and leading to the most stable structures are shown in [Table 7](#).

Two structures are obtained from the interaction of the most stable water pentamer with the solute:  $TS_1^{W5,A}$  and  $TS_3^{W5,A}$ . In the previous cases, interactions with several smaller water clusters were also investigated, and the most stable one consists of a water dimer and a water trimer interacting with  $TS_1$  (structure  $TS_2^{W5,A}$ ).

The  $TS_1^{W5,A}$  structure is the most stable one obtained and it is characterized by a strong deformation of the flat structure of the water pentamer. This structure lies 81.72 kJ/mol below the five water molecules and the reagents taken separately.

In the  $TS_3^{W5,A}$  structure, the water pentamer is less distorted, but the water-solute interactions are weaker and as a result this structure is about 20 kJ/mol less stable than the first one, at 62.07 kJ/mol below the isolated partners.

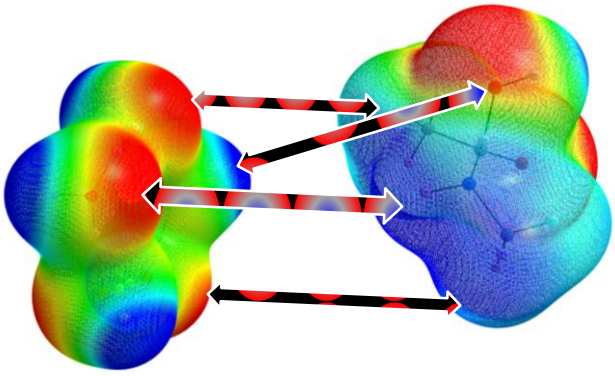
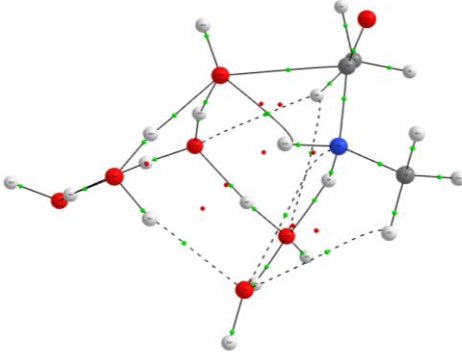
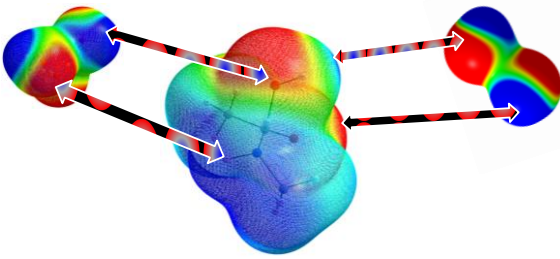
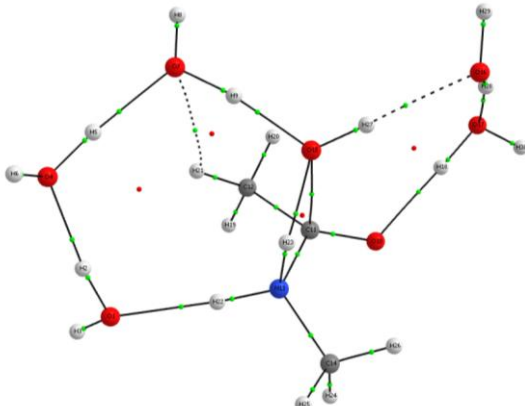
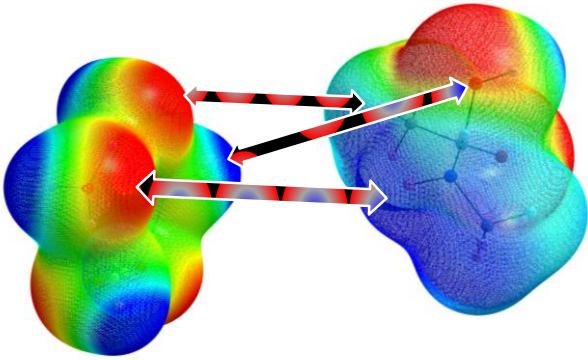
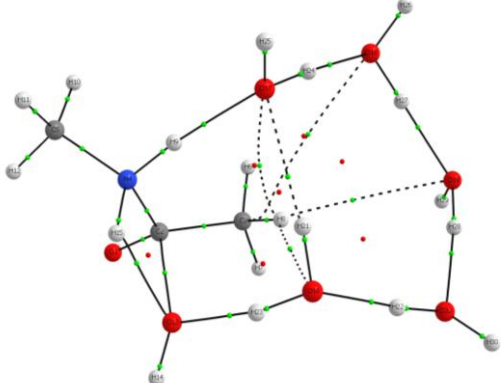
Alternatively, the separate interaction of a water dimer and a water trimer with the non-hydrated TS leads to the  $TS_2^{W5,A}$  structure:

- a water dimer interacts with the oxygen atom of the carbonyl group and with the hydrogen atom of the OH group,



- simultaneously a water trimer interacts with the oxygen atom of the OH group and with the hydrogen atom of the amine group.

It is interesting to note that this  $TS_2^{W5\_A}$  structure is located 63.90 kJ/mol below the isolated partners, and is almost isoenergetic with the  $TS_3^{W5\_A}$  structure.

Considered direction of approach on the basis on the MESP analysis	Structures and energies of the optimized microhydrated transition states
	 $\Delta E = -81.72 \text{ kJ/mol. } TS_1^{W5\_A}$
	 $\Delta E = -63.90 \text{ kJ/mol. } TS_2^{W5\_A}$
	 $\Delta E = -62.07 \text{ kJ/mol. } TS_3^{W5\_A}$

**Table 7: Microhydration of the  $TS_1$  with five water molecule: Identification of possible directions of approaches from the MESP, and structures and energies of the optimized microhydrated transition states.**

The reaction path associated with the most stable TS ( $TS_1^{W5\_A}$ ) is shown in [Figure 13](#). As in the most energetically favorable reaction mechanisms obtained with fewer water molecules, the interaction between water and TS leads to the formation of two particularly important hydrogen bondings, involving the hydrogen atom of the amine function, which is a priori not directly involved in the reaction, and the oxygen atom leading to the loss of the water molecule. A network of hydrogen bonding is created between these two sites via the water cluster.

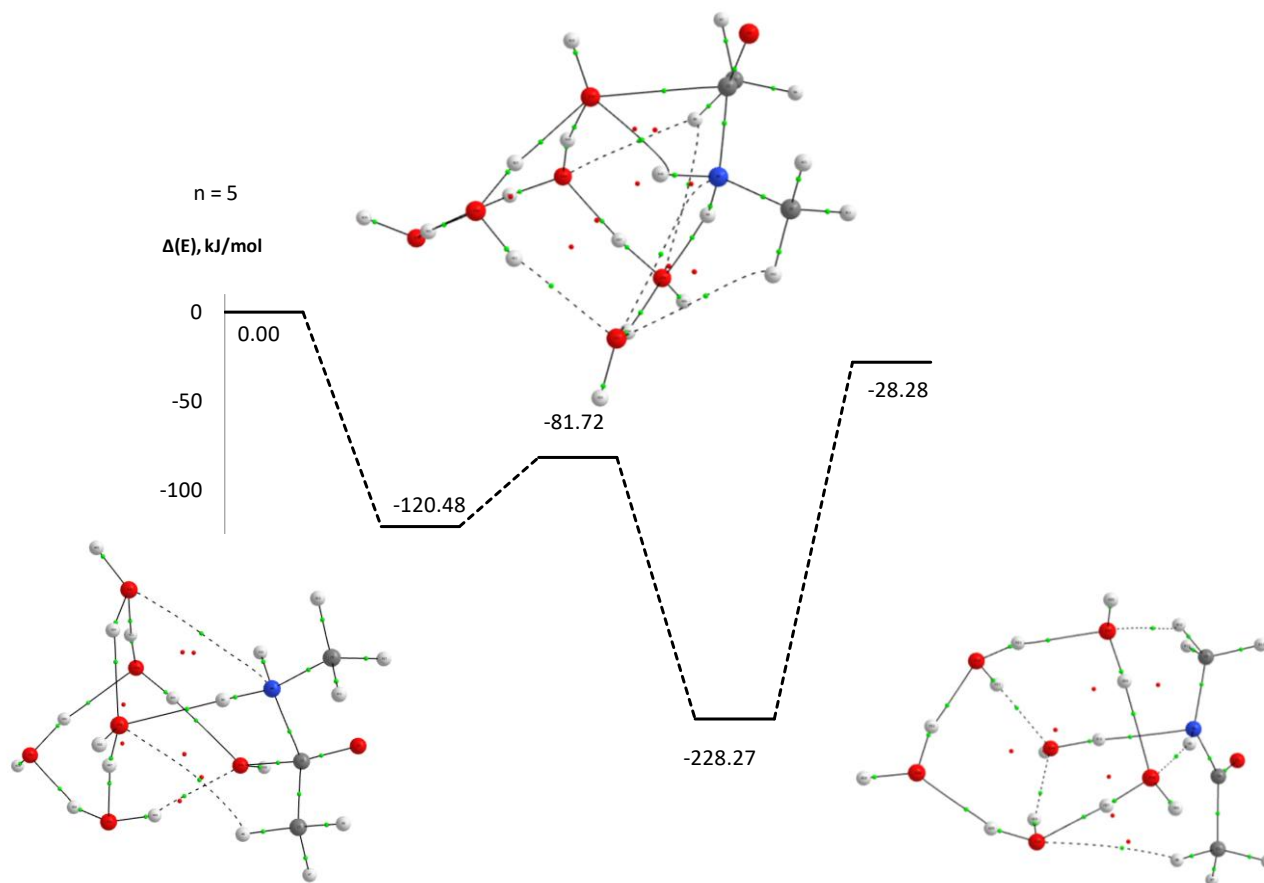


**Figure 13: Energy profile for the peptide-like bond formation reaction involving the most stable transition state with five water molecules identified ( $TS_1^{W5\_A}$ ).**

It is worth mentioning that in all the cases presented below, the motion associated with the imaginary frequency of the TS has been identified as indeed corresponding to the reaction process, and all the reaction paths have been obtained by performing IRC calculations from the identified transition states.

#### *Microhydration of one of the reagents prior to the formation of a $(CH_3COOH)(CH_3NH_2)(H_2O)_n$ complex*

Alternatively, the second approach we have considered is to search for possible reaction pathways from the most stable microhydrated complexes.

It is worth mentioning that all the studies reported in the literature use this type of approach: the search for the most stable pre-reactive complexes, followed by the identification of the associated reaction pathways. Since this type of approach is widely used, we only present here the main steps

and specific features of our study, and all the structures identified are presented in Supporting Information.

Two partners, either  $(\text{CH}_3\text{COOH})(\text{H}_2\text{O})_n$  and  $(\text{CH}_3\text{NH}_2)$ , or  $(\text{CH}_3\text{COOH})$  and  $(\text{CH}_3\text{NH}_2)(\text{H}_2\text{O})_n$ , or  $(\text{CH}_3\text{COOH})(\text{H}_2\text{O})_x$  and  $(\text{CH}_3\text{NH}_2)(\text{H}_2\text{O})_y$ , with  $x + y = n$ , can be obtained. The MESP analyses of these couples of partners allow to identify preferential approaches that may lead to the maximization of interactions between their complementary sites. The most favorable microhydrated complexes  $(\text{CH}_3\text{COOH})(\text{CH}_3\text{NH}_2)(\text{H}_2\text{O})_n$  for  $1 \leq n \leq 5$  have thus been identified, and the potential energy surfaces obtained are presented in Supporting Information. An example is shown in [Figure 14](#), in the case of the  $(\text{CH}_3\text{COOH}):(\text{H}_2\text{O})$  complex interacting with methylamine.

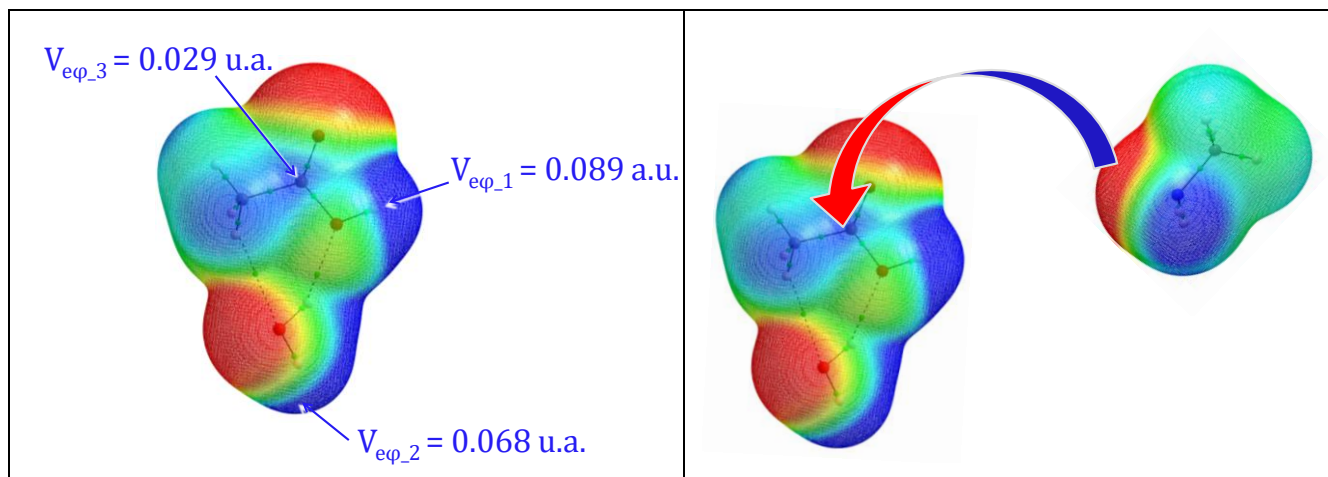


**Figure 14: MESP analysis of the  $(\text{CH}_3\text{COOH}):(\text{H}_2\text{O})$  complex, and identification of a preferential direction of approach of the methylamine that may lead to the formation of the peptide-like bond.**

In the most stable monohydrated complex, the water molecule acts as a hydrogen bond donor with the oxygen atom of the  $\text{C}=\text{O}$  functional group and as a hydrogen bond acceptor, with the hydrogen atom of the  $\text{OH}$  functional group of acetic acid. The corresponding non-covalent  $(\text{NH}_2\text{CH}_3):(\text{CH}_3\text{COOH}):(\text{H}_2\text{O})$  complex is located 52.61 kJ/mol below the three partners taken separately. The transition state subsequently obtained leads to the formation of a water dimer interacting with the product. The transition state corresponds to the migration of one hydrogen atom of the amine towards the oxygen atom of the  $\text{OH}$  group, with the concomitant formation of the  $\text{C}-\text{N}$  bond and the rupture of the  $\text{C}-\text{O}$  bond. The energy barrier associated with this transition state is 110.08 kJ/mol ([Figure 15](#)).

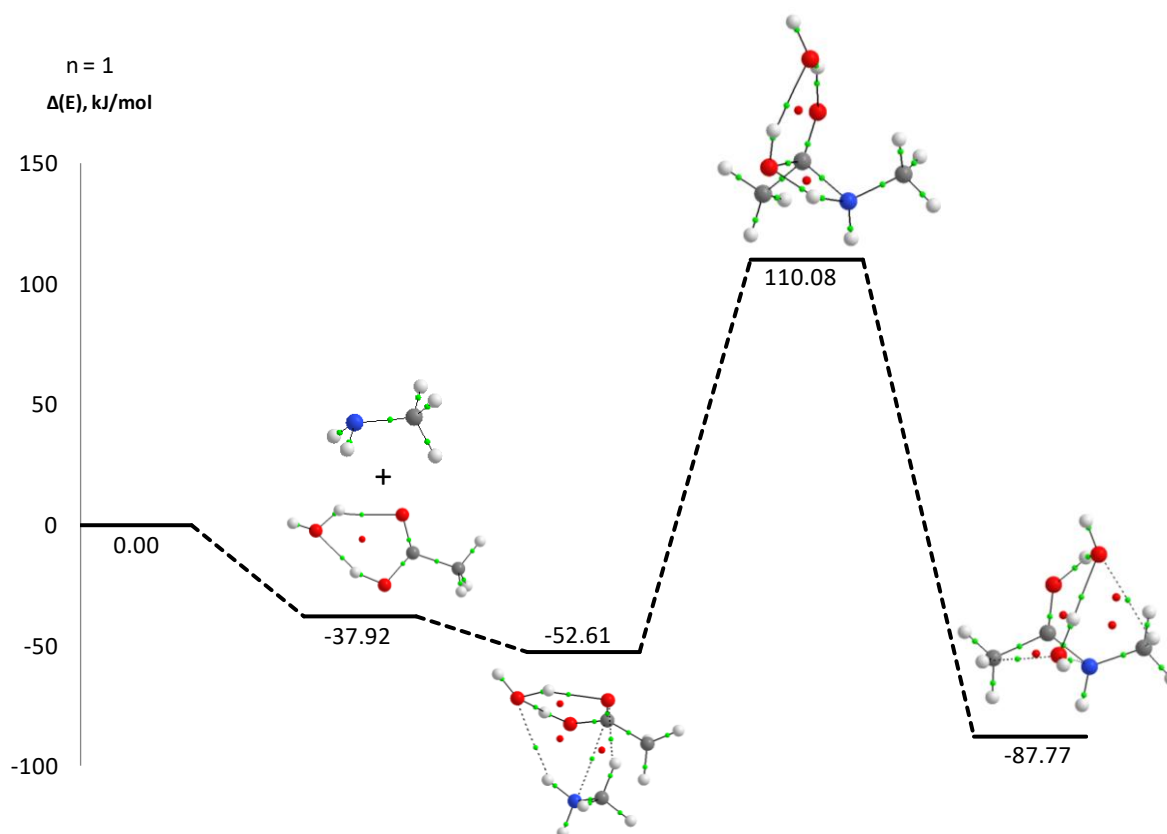


**Figure 15: Energy profile for the peptide-like bond formation reaction involving the most stable pre-reactive monohydrated complex identified.**

This pre-reactive non-covalent complex  $(\text{NH}_2\text{CH}_3):(\text{CH}_3\text{COOH}):(\text{H}_2\text{O})$  is approximately 20 kJ/mol more stable than the one involved in the reaction mechanism shown in [Figure 7](#) ( $\Delta E$  of -52.61 kJ/mol and -33.09 kJ/mol, respectively). On the other hand, the energy barrier that has to be overcome to lead to the formation of  $(\text{CH}_3\text{CONHCH}_3):(\text{H}_2\text{O})_2$  is approximately 15 kJ/mol higher ( $\Delta E$  of +110.08 kJ/mol and +96.93 kJ/mol, respectively).

Finally, the potential energy surfaces thus obtained in the presence of one to five water molecules are presented in Supplementary Information. It is worth emphasizing that the energy barriers associated with these reaction pathways are systematically higher than those obtained from the microhydration of the transition state.

### Discussion

The diagram shown in [Figure 16](#) allows to compare the energy barriers of the reaction pathways obtained by both approaches, as a function of the number of microhydration water molecules. It can be seen that the microhydration of the transition state obtained in the case of the reaction without water molecules systematically leads to the most favourable reaction pathways from an energy point of view. Furthermore, from three water molecules, a barrierless reaction is identified for the formation of the peptide-like bond between  $\text{CH}_3\text{COOH}$  and  $\text{NH}_2\text{CH}_3$ .

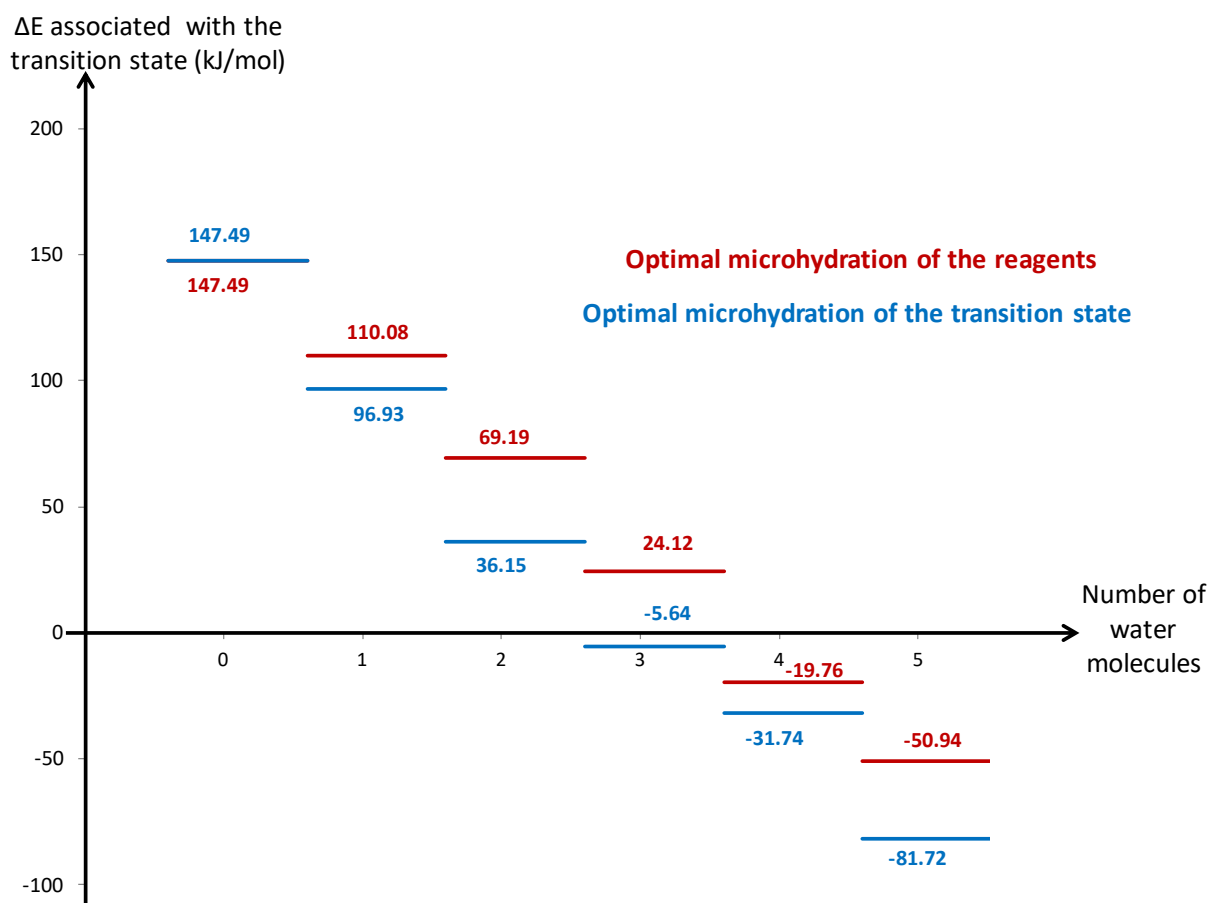


**Figure 16: Comparison of the energy barriers of the reaction pathways obtained by studying either the microhydration of the reagents (in red) or the microhydration of the transition state (in blue), as a function of the number of water molecules.**

As we already mentioned, other studies in literature have focused on the influence of microhydration on the reaction of such compounds, amines, carboxylic acids, amides or ketones. In particular, G. Bouchoux et al.<sup>4</sup> showed that, in the case of Strecker synthesis from ammonia and formaldehyde, water molecules could play either an "active catalyst" or a "passive catalyst" role:

- the water molecules acting as an "active catalyst" are directly involved in the proton transfer process between the two reactants, via the formation of a "chain of hydrogen bonds" along which the proton transfer propagates,
- water molecules acting as a "passive catalyst" form hydrogen bond interactions without being directly involved in hydrogen atom transfer.

In the case of the formation of a peptide-like bond between acetic acid and methylamine, it seems that the formation of a hydrogen bond network between the hydrogen atom of the methylamine that is not directly involved in the reaction and the oxygen atom leading to the loss of the water molecule promotes the reaction.

### Conclusion

The MESP study of methylamine and acetic acid allowed the identification of preferential directions of approach of the two partners and different non-covalent complexes were identified. One of these complexes, having a complexation energy of 14.22 kJ/mol, may correspond to a preliminary step in the reaction leading to the formation of the peptide-like bond. The energy barrier associated with

this reaction is calculated as being 147.49 kJ/mol. therefore , this reaction cannot take place spontaneously.

The formation of microhydrated complexes was then studied, from the MESP analysis, by identifying preferential directions of approach of water molecules with respect to the reagents, or with respect to the transition state, by maximizing interactions between complementary sites. In each case, it was possible to identify a microhydrated  $(\text{NH}_2\text{CH}_3):(\text{CH}_3\text{COOH}):(\text{H}_2\text{O})_{1\leq n\leq 5}$  complex as a preliminary step toward the reaction. The transition states associated with these reactions of peptide-like bond formation in the presence of microhydration were identified. It was found that water molecules could:

- either interact with the carboxylic acid group of acetic acid: this type of structure corresponds to the formation of the most stable pre-reactive  $(\text{NH}_2\text{CH}_3):(\text{CH}_3\text{COOH}):(\text{H}_2\text{O})_{1\leq n\leq 5}$  complexes and they are obtained by seeking to maximize the interactions between the reagents and the water molecules,
- or form a network of hydrogen bonds linking one of the hydrogen atoms of the amine function with the oxygen atom involved in the loss of the water molecule: this type of structure corresponds to the reaction mechanisms associated with the lowest energy barriers, and is obtained by seeking to maximize interactions between water molecules and the transition state identified for the reaction without any water molecules.

To conclude, this work suggests that, in the gas phase, the combined MESP study, the maximization of interactions between complementary sites, geometry optimizations and IRC calculations, and the QTAIM analysis of the structures obtained, constitutes an interesting approach to characterize at the same time non-covalent complexes, transition states and reaction pathways. This work also suggests that a C-N bond could be formed from acetic acid and methylamine taken in their fundamental states, in the presence of a small number of water molecules. Following a preliminary study using a mass spectrometer coupled with the synchrotron radiations,<sup>92</sup> we will further investigate this aspect from an experimental point of view.

---

<sup>1</sup> Perez, J. E., Kumar, M., Francisco, J. S., & Sinha, A. (2017). Oxygenate-Induced Tuning of Aldehyde-Amine Reactivity and Its Atmospheric Implications. *The Journal of Physical Chemistry A*, 121(5), 1022-1031.

<sup>2</sup> Dong, Z. G., Xu, F., & Long, B. (2018). The energetics and kinetics of the  $\text{CH}_3\text{CHO}+(\text{CH}_3)_2\text{NH}/\text{CH}_3\text{NH}_2$  reactions catalyzed by a single water molecule in the atmosphere. *Computational and Theoretical Chemistry*, 1140, 7-13.

<sup>3</sup> Louie, M. K., Francisco, J. S., Verdicchio, M., Klippenstein, S. J., & Sinha, A. (2016). Dimethylamine addition to formaldehyde catalyzed by a single water molecule: a facile route for atmospheric carbinolamine formation and potential promoter of aerosol growth. *The Journal of Physical Chemistry A*, 120(9), 1358-1368.

<sup>4</sup> Riffet, V., Frison, G., & Bouchoux, G. (2018). Quantum-chemical modeling of the first steps of the Strecker synthesis: from the gas-phase to water solvation. *The Journal of Physical Chemistry A*, 122(6), 1643-1657.

- 
- <sup>5</sup> Tan, X. F., Zhang, L., & Long, B. (2020). New mechanistic pathways for the formation of organosulfates catalyzed by ammonia and carbinolamine formation catalyzed by sulfuric acid in the atmosphere. *Physical Chemistry Chemical Physics*, 22(16), 8800-8807.
- <sup>6</sup> Liu, J. Y., Long, Z. W., Mitchell, E., & Long, B. (2021). New Mechanistic Pathways for the Reactions of Formaldehyde with Formic Acid Catalyzed by Sulfuric Acid and Formaldehyde with Sulfuric Acid Catalyzed by Formic Acid: Formation of Potential Secondary Organic Aerosol Precursors. *ACS Earth Space Chem.* 2021, 5, 6, 1363–1372
- <sup>7</sup> Dong, Z. G., Xu, F., & Long, B. (2018). The energetics and kinetics of the  $\text{CH}_3\text{CHO}+(\text{CH}_3)_2\text{NH}/\text{CH}_3\text{NH}_2$  reactions catalyzed by a single water molecule in the atmosphere. *Computational and Theoretical Chemistry*, 1140, 7-13.
- <sup>8</sup> Galloway, M. M., Powelson, M. H., Sedehi, N., Wood, S. E., Millage, K. D., Kononenko, J. A., Rynaski, A. D. & De Haan, D. O. (2014). Secondary organic aerosol formation during evaporation of droplets containing atmospheric aldehydes, amines, and ammonium sulfate. *Environmental science & technology*, 48(24), 14417-14425.
- <sup>9</sup> Dong, Z. G., Xu, F., Mitchell, E., & Long, B. (2021). Trifluoroacetaldehyde aminolysis catalyzed by a single water molecule: An important sink pathway for trifluoroacetaldehyde and a potential pathway for secondary organic aerosol growth. *Atmospheric Environment*, 249, 118242.
- <sup>10</sup> Colzi, L., Rivilla, V. M., Beltrán, M. T., Jiménez-Serra, I., Mininni, C., Melosso, M., Cesaroni, R., Fontani, F., Lorenzani, A., Sanchez-Monge, A. et al. (2021). The GUAPOS project II. A comprehensive study of peptide-like bond molecules. *arXiv preprint arXiv:2107.11258*.
- <sup>11</sup> Georgelin, T., Jaber, M., Bazzi, H., & Lambert, J. F. (2013). Formation of activated biomolecules by condensation on mineral surfaces—a comparison of peptide bond formation and phosphate condensation. *Origins of Life and Evolution of Biospheres*, 43(4), 429-443.
- <sup>12</sup> Rimola, A., Tosoni, S., Sodupe, M., & Ugliengo, P. (2006). Does Silica Surface Catalyse Peptide Bond Formation? New Insights from First-Principles Calculations. *ChemPhysChem*, 7(1), 157-163
- <sup>13</sup> Rimola, A., Sodupe, M., & Ugliengo, P. (2019). Role of mineral surfaces in prebiotic chemical evolution. In silico quantum mechanical studies. *Life*, 9(1), 10.
- <sup>14</sup> Georgelin, T., Akouche, M., Jaber, M., Sakhno, Y., Matheron, L., Fournier, F., Méthivier, C., Martra, G. & Lambert, J. F. (2017). Iron (III) oxide nanoparticles as catalysts for the formation of linear glycine peptides. *European Journal of Inorganic Chemistry*, 2017(1), 198-211.
- <sup>15</sup> Tielens, F., Gierada, M., Handzlik, J., & Calatayud, M. (2020). Characterization of amorphous silica based catalysts using DFT computational methods. *Catalysis Today*, 354, 3-18.
- <sup>16</sup> Pantaleone, S., Ugliengo, P., Sodupe, M., & Rimola, A. (2018). When the surface matters: prebiotic peptide-bond formation on the  $\text{TiO}_2$  (101) anatase surface through periodic DFT-D2 simulations. *Chem. Eur. J.*, 24, 16292-16301.
- <sup>17</sup> Rufino, V. C., & Pliego Jr, J. R. (2020). The role of carboxylic acid impurity in the mechanism of the formation of aldimines in aprotic solvents. *Computational and Theoretical Chemistry*, 1191, 113053.

- 
- <sup>18</sup> Parr, R. G., & Yang, W. (1995). Density-functional theory of the electronic structure of molecules. *Annual review of physical chemistry*, 46(1), 701-728.
- <sup>19</sup> Parr, R. G., & Yang, W. (1984). Density functional approach to the frontier-electron theory of chemical reactivity. *Journal of the American Chemical Society*, 106(14), 4049-4050.
- <sup>20</sup> Chermette, H. (1999). Chemical reactivity indexes in density functional theory. *J. Comput. Chem.*, 20, 129–154
- <sup>21</sup> Politzer, P., & Murray, J. S. (2020). Electrostatics and Polarization in  $\sigma$ - and  $\pi$ -Hole Noncovalent Interactions: An Overview. *ChemPhysChem*, 21(7), 579-588.
- <sup>22</sup> Politzer, P., Murray, J. S., & Clark, T. (2019). Explicit inclusion of polarizing electric fields in  $\sigma$ - and  $\pi$ -hole interactions. *The Journal of Physical Chemistry A*, 123(46), 10123-10130.
- <sup>23</sup> Frontera, A., & Bauzá, A. (2017). Concurrent aerogen bonding and lone pair/anion- $\pi$  interactions in the stability of organoxenon derivatives: A combined CSD and ab initio study. *Physical Chemistry Chemical Physics*, 19(44), 30063-30068.
- <sup>24</sup> Bijina, P. V., & Suresh, C. H. (2020). Molecular electrostatic potential reorganization theory to describe positive cooperativity in noncovalent trimer complexes. *The Journal of Physical Chemistry A*, 124(11), 2231-2241.
- <sup>25</sup> Anjali, B. A., & Suresh, C. H. (2020). Absorption and emission properties of 5-phenyl tris (8-hydroxyquinolino) M (III) complexes (M= Al, Ga, In) and correlations with molecular electrostatic potential. *Journal of computational chemistry*, 41(16), 1497-1508.
- <sup>26</sup> Sosorev, A., Dominskiy, D., Chernyshov, I., & Efremov, R. (2020). Tuning of Molecular Electrostatic Potential Enables Efficient Charge Transport in Crystalline Azaacenes: A Computational Study. *International journal of molecular sciences*, 21(16), 5654.
- <sup>27</sup> Gadre, S. R., Suresh, C. H., & Mohan, N. (2021). Electrostatic Potential Topology for Probing Molecular Structure, Bonding and Reactivity. *Molecules*, 26(11), 3289.
- <sup>28</sup> Pundlik, S. S., & Gadre, S. R. (1997). Structure and stability of DNA base trimers: an electrostatic approach. *J. Phys. Chem. B*, 101(46), 9657-9662.
- <sup>29</sup> Gadre, S. R., & Bhadane, P. K. (1997). Patterns in hydrogen bonding via electrostatic potential topography. *J. Chem. Phys.*, 107(14), 5625-5626.
- <sup>30</sup> Mohan, N., Suresh, C. H., Kumar, A., & Gadre, S. R. (2013). Molecular electrostatics for probing lone pair- $\pi$  interactions. *Phys. Chem. Chem. Phys.*, 15(42), 18401-18409.
- <sup>31</sup> Gadre, S. R., & Kumar, A. (2015). Understanding lone pair- $\pi$  interactions from electrostatic viewpoint. In *Noncovalent Forces* (pp. 391-418). Springer, Cham.
- <sup>32</sup> Kulkarni, A. D., Babu, K., Gadre, S. R., & Bartolotti, L. J. (2004). Exploring hydration patterns of aldehydes and amides: Ab initio investigations. *J. Phys. Chem. A*, 108(13), 2492-2498.
- <sup>33</sup> Ayers, P. W. (2001). Strategies for computing chemical reactivity indices. *Theoretical Chemistry Accounts*, 106(4), 271-279.
- <sup>34</sup> Geerlings, P., Ayers, P. W., Toro-Labbé, A., Chattaraj, P. K., & De Proft, F. (2012). The Woodward–Hoffmann rules reinterpreted by conceptual density functional theory. *Accounts of chemical research*, 45(5), 683-695.



- 
- <sup>35</sup> Geerlings, P., et al. (2020). Conceptual density functional theory: status, prospects, issues. *Theoretical Chemistry Accounts*, 139(2), 1-18.
- <sup>36</sup> Bacchus-Montabonel, M. C., & Calvo, F. Nanohydration of uracil: Emergence of Three-Dimensional Structures and Proton-Induced Charge Transfer, *Phys. Chem. Chem. Phys.* 2015, 17, 9629-9633.
- <sup>37</sup> Pérez, C., Neill, J. L., Muckle, M. T., Zaleski, D. P., Peña, I., Lopez, J. C., ... & Pate, B. H. (2015). Water–water and water–solute interactions in microsolvated organic complexes. *Angewandte Chemie International Edition*, 54(3), 979-982.
- <sup>38</sup> Blanco, S., Pinacho, P., & López, J. C. (2017). Structure and Dynamics in Formamide–(H<sub>2</sub>O) 3: A Water Pentamer Analogue. *The journal of physical chemistry letters*, 8(24), 6060-6066.
- <sup>39</sup> Gruet, S., Pérez, C., Steber, A. L., & Schnell, M. (2018). Where's water? The many binding sites of hydantoin. *Physical Chemistry Chemical Physics*, 20(8), 5545-5552.
- <sup>40</sup> Derbali, I., Thissen, R., Alcaraz, C., Romanzin, C., Zins, E.L. Study of the Reactivity of CH<sub>3</sub>COOH<sup>+</sup> and COOH<sup>+</sup> Ions With CH<sub>3</sub>NH<sub>2</sub> : Evidence of the Formation of New Peptide-like C(O)-N Bonds. Manuscript No.: jp-2021-06630q Accepted for publication in The Journal of Physical Chemistry A.
- <sup>41</sup> Sun, F., Xie, M., Zhang, Y., Song, W., Sun, X., & Hu, Y. (2021). Spectroscopic evidence of the C–N covalent bond formed between two interstellar molecules (ISM): acrylonitrile and ammonia. *Physical Chemistry Chemical Physics*.
- <sup>42</sup> Jeanvoine, Y., Largo, A., Hase, W. L., & Spezia, R. (2018). Gas phase synthesis of protonated glycine by chemical dynamics simulations. *The Journal of Physical Chemistry A*, 122(3), 869-877.
- <sup>43</sup> Scuderi, D., Pérez-Mellor, A., Lemaire, J., Indrajith, S., Bardaud, J. X., Largo, A., Jeanvoine Y. & Spezia, R. (2020). Infrared-Assisted Synthesis of Prebiotic Glycine. *ChemPhysChem*, 21(6), 503-509.
- <sup>44</sup> Enrique-Romero, J., Rimola, A., Ceccarelli, C., Ugliengo, P., Balucani, N., & Skouteris, D. (2019). Reactivity of HCO with CH<sub>3</sub> and NH<sub>2</sub> on Water Ice Surfaces. A Comprehensive Accurate Quantum Chemistry Study. *ACS Earth and Space Chemistry*, 3(10), 2158-2170.
- <sup>45</sup> van der Rest, G., Jensen, L. B., Azeim, S. A., Mourgues, P., & Audier, H. E. (2004). Reactions of [NH<sub>3</sub><sup>+</sup>, H<sub>2</sub>O] with carbonyl compounds: a McLafferty rearrangement within a complex?. *Journal of the American Society for Mass Spectrometry*, 15(7), 966-971.
- <sup>46</sup> van der Rest, G., Mourgues, P., Nedev, H., & Audier, H. E. (2002). A prototype for catalyzed amide bond cleavage: production of the [NH<sub>3</sub>, H<sub>2</sub>O]<sup>++</sup> dimer from ionized formamide and its carbene isomer. *Journal of the American Chemical Society*, 124(19), 5561-5569.
- <sup>47</sup> Politzer P, Murray JS (2018) The Hellmann-Feynman theorem: a perspective. *J. Mol. Model.* 24(9):266
- <sup>48</sup> Bader, R. F., Carroll, M. T., Cheeseman, J. R., & Chang, C. (1987). Properties of atoms in molecules: atomic volumes. *J. Am. chem. Soc.*, 109(26), 7968-7979.
- <sup>49</sup> Politzer, P., Murray, J. S., & Clark, T. (2015). Mathematical modeling and physical reality in noncovalent interactions. *Journal of molecular modeling*, 21(3), 1-10.
- <sup>50</sup> Herbert, J. M. (2021). Neat, Simple, and Wrong: Debunking Electrostatic Fallacies Regarding Noncovalent Interactions. *The Journal of Physical Chemistry A*.

- 
- <sup>51</sup> Gadre, S. R., Babu, K., & Rendell, A. P. (2000). Electrostatics for exploring hydration patterns of molecules. 3. Uracil. *J. Phys. Chem. A*, *104*(39), 8976-8982.
- <sup>52</sup> Sivanesan, D., Babu, K., Gadre, S. R., Subramanian, V., & Ramasami, T. (2000). Does a stacked DNA base pair hydrate better than a hydrogen-bonded one? An ab initio study. *J. Phys. Chem. A*, *104*(46), 10887-10894.
- <sup>53</sup> Güssregen, S., Matter, H., Hessler, G., Müller, M., Schmidt, F., & Clark, T. (2012). 3D-QSAR based on quantum-chemical molecular fields: toward an improved description of halogen interactions. *Journal of chemical information and modeling*, *52*(9), 2441-2453.
- <sup>54</sup> El Kerdawy, A., Güssregen, S., Matter, H., Hennemann, M., & Clark, T. (2013). Quantum mechanics-based properties for 3D-QSAR. *Journal of chemical information and modeling*, *53*(6), 1486-1502.
- <sup>55</sup> El Kerdawy, A., Wick, C. R., Hennemann, M., & Clark, T. (2012). Predicting the sites and energies of noncovalent intermolecular interactions using local properties. *Journal of chemical information and modeling*, *52*(4), 1061-1071.
- <sup>56</sup> Gaussian 09, Revision D.01, M. J. Frisch, G. W. Trucks, H. B. Schlegel, G. E. Scuseria, M. A. Robb, J. R. Cheeseman, G. Scalmani, V. Barone, G. A. Petersson, H. Nakatsuji, X. Li, M. Caricato, A. Marenich, J. Bloino, B. G. Janesko, R. Gomperts, B. Mennucci, H. P. Hratchian, J. V. Ortiz, A. F. Izmaylov, J. L. Sonnenberg, D. Williams-Young, F. Ding, F. Lipparini, F. Egidi, J. Goings, B. Peng, A. Petrone, T. Henderson, D. Ranasinghe, V. G. Zakrzewski, J. Gao, N. Rega, G. Zheng, W. Liang, M. Hada, M. Ehara, K. Toyota, R. Fukuda, J. Hasegawa, M. Ishida, T. Nakajima, Y. Honda, O. Kitao, H. Nakai, T. Vreven, K. Throssell, J. A. Montgomery, Jr., J. E. Peralta, F. Ogliaro, M. Bearpark, J. J. Heyd, E. Brothers, K. N. Kudin, V. N. Staroverov, T. Keith, R. Kobayashi, J. Normand, K. Raghavachari, A. Rendell, J. C. Burant, S. S. Iyengar, J. Tomasi, M. Cossi, J. M. Millam, M. Klene, C. Adamo, R. Cammi, J. W. Ochterski, R. L. Martin, K. Morokuma, O. Farkas, J. B. Foresman, and D. J. Fox, Gaussian, Inc., Wallingford CT, 2016.
- <sup>57</sup> Vydrov, O.A., & Scuseria, G.E. (2006) Assessment of a long-range corrected hybrid functional. *J. Chem.Phys.* *125*(23):234109
- <sup>58</sup> Vydrov, O.A., Heyd, J., Krukau, A.V., & Scuseria, G.E. (2006) Importance of short-range versus long-range Hartree-Fock exchange for the performance of hybrid density functionals. *J. Chem.Phys.* *125*(7):074106
- <sup>59</sup> Vydrov, O.A., Scuseria, G.E., & Perdew, J.P. (2007) Tests of functionals for systems with fractional electron number. *J. Chem.Phys.* *126*(15):154109
- <sup>60</sup> Grimme, S., Ehrlich, S., & Goerigk, L. (2011). Effect of the damping function in dispersion corrected density functional theory. *Journal of computational chemistry*, *32*(7), 1456-1465.
- <sup>61</sup> Krishnan, R. B. J. S., Binkley, J. S., Seeger, R., & Pople, J. A. (1980). Self-consistent molecular orbital methods. XX. A basis set for correlated wave functions. *The Journal of chemical physics*, *72*(1), 650-654.
- <sup>62</sup> Goerigk, L., Kruse, H., & Grimme, S. (2011). Benchmarking density functional methods against the S66 and S66x8 datasets for non-covalent interactions. *ChemPhysChem*, *12*(17), 3421-3433.
- <sup>63</sup> DiLabio, G. A., Johnson, E. R., & Otero-de-la-Roza, A. (2013). Performance of conventional and dispersion-corrected density-functional theory methods for hydrogen bonding interaction energies. *Physical Chemistry Chemical Physics*, *15*(31), 12821-12828.

- 
- <sup>64</sup> Bader RF, Streitwieser A, Neuhaus A, Laidig KE, Speers P (1996) Electron delocalization and the Fermi hole. *J. Am. Chem. Soc.* 118(21):4959–4965.
- <sup>65</sup> Wick, C. R., & Clark, T. (2018). On bond-critical points in QTAIM and weak interactions. *Journal of molecular modeling*, 24(6), 1-9.
- <sup>66</sup> Jabłoński, M. (2020). Counterintuitive bond paths: An intriguing case of the C (NO<sub>2</sub>)<sup>3-</sup> ion. *Chemical Physics Letters*, 759, 137946.
- <sup>67</sup> Jabłoński, M. (2019). On the uselessness of bond paths linking distant atoms and on the violation of the concept of privileged exchange channels. *ChemistryOpen*, 8(4), 497.
- <sup>68</sup> Suvitha, A., Venkataramanan, N. S., Sahara, R., & Kawazoe, Y. (2019). A theoretical exploration of the intermolecular interactions between resveratrol and water: a DFT and AIM analysis. *Journal of molecular modeling*, 25(3), 1-11.
- <sup>69</sup> Venkataramanan, N. S., Suvitha, A., & Kawazoe, Y. (2017). Intermolecular interaction in nucleobases and dimethyl sulfoxide/water molecules: A DFT, NBO, AIM and NCI analysis. *Journal of Molecular Graphics and Modelling*, 78, 48-60.
- <sup>70</sup> Sathiyamoorthy, V. N. (2021). Electronic structure, stability, and cooperativity of chalcogen bonding in sulfur dioxide and hydrated sulfur dioxide clusters: a DFT study and wave functional analysis.
- <sup>71</sup> Grabowski, S. J., & Leszczynski, J. (2009). The enhancement of X–H... π hydrogen bond by cooperativity effects—Ab initio and QTAIM calculations. *Chemical Physics*, 355(2-3), 169-176.
- <sup>72</sup> Derbali, I., Zins, E. L., & Alikhani, M. E. (2019). What is the hydrophobic interaction contribution to the stabilization of micro-hydrated complexes of trimethylamine oxide (TMAO)? A joint DFT-D, QTAIM, and MESP study. *Journal of molecular modeling*, 25(12), 1-14.
- <sup>73</sup> Zins, E. L. (2020). Microhydration of a Carbonyl Group: How does the Molecular Electrostatic Potential (MESP) Impact the Formation of (H<sub>2</sub>O) <sub>n</sub>:(R<sub>2</sub>C=O) Complexes?. *The Journal of Physical Chemistry A*, 124(9), 1720-1734.
- <sup>74</sup> Gao, J., Seifert, N. A., & Jäger, W. (2019). A microwave spectroscopic and ab initio study of keto–enol tautomerism and isomerism in the cyclohexanone–water complex. *Physical Chemistry Chemical Physics*, 21(24), 12872-12880.
- <sup>75</sup> Weinhold, F., & Klein, R. A. (2012). What is a hydrogen bond? Mutually consistent theoretical and experimental criteria for characterizing H-bonding interactions. *Molecular Physics*, 110(9-10), 565-579.
- <sup>76</sup> Akman, F., Issaoui, N., & Kazachenko, A. S. (2020). Intermolecular hydrogen bond interactions in the thiourea/water complexes (Thio-(H<sub>2</sub>O) <sub>n</sub>)(n = 1,..., 5): X-ray, DFT, NBO, AIM, and RDG analyses. *Journal of Molecular Modeling*, 26, 1-16.
- <sup>77</sup> Grabowski, S. J. (2020). Triel bond and coordination of triel centres—Comparison with hydrogen bond interaction. *Coordination Chemistry Reviews*, 407, 213171.
- <sup>78</sup> Scheiner, S., Michalczyk, M., Wysokiński, R., & Zierkiewicz, W. (2020). Structures and energetics of clusters surrounding diatomic anions stabilized by hydrogen, halogen, and other noncovalent bonds. *Chemical Physics*, 530, 110590.

- <sup>79</sup> Gholami, S., Aarabi, M., & Grabowski, S. J. (2021). Coexistence of Intra-and Intermolecular Hydrogen Bonds: Salicylic Acid and Salicylamide and Their Thiol Counterparts. *The Journal of Physical Chemistry A*, 125(7), 1526-1539.
- <sup>80</sup> Hobza P, Müller-Dethlefs K (2010) Non-covalent interactions: theory and experiment (No. 2). Royal Society of Chemistry
- <sup>81</sup> Gadre SR, Yeole SD, Sahu N (2014) Chem Rev 114:12132–12173 20. Murray JS, Sen K (1996) Molecular electrostatic potentials: concepts and applications. Elsevier Science, Amsterdam.
- <sup>82</sup> Kolar, M. H., & Hobza, P. (2016). Computer modeling of halogen bonds and other  $\sigma$ -hole interactions. *Chemical reviews*, 116(9), 5155-5187.
- <sup>83</sup> Bauzá, A., Mooibroek, T. J., & Frontera, A. (2015). The Bright Future of Unconventional  $\sigma/\pi$ -Hole Interactions. *ChemPhysChem*, 16(12), 2496-2517.
- <sup>84</sup> Remya, K., & Suresh, C. H. (2015). Non-covalent intermolecular carbon–carbon interactions in polyynes. *Physical Chemistry Chemical Physics*, 17(40), 27035-27044.
- <sup>85</sup> Lv, S. S., Liu, Y. R., Huang, T., Feng, Y. J., Jiang, S., & Huang, W. (2015). Stability of hydrated methylamine: Structural characteristics and H<sub>2</sub>N... H–O hydrogen bonds. *The Journal of Physical Chemistry A*, 119(16), 3770-3779.
- <sup>86</sup> Krishnakumar, P., & Maity, D. K. (2017). Microhydration of Neutral and Charged Acetic Acid. *The Journal of Physical Chemistry A*, 121(2), 493-504.
- <sup>87</sup> Kang, N. S., & Kang, Y. K. (2017). Assessment of CCSD (T), MP2, and DFT methods for the calculations of structures and interaction energies of the peptide backbone with water molecules. *Chemical Physics Letters*, 687, 23-30.
- <sup>88</sup> Calvo, F., & Bacchus-Montabonel, M. C. (2018). Size-Induced Segregation in the Stepwise Microhydration of Hydantoin and Its Role in Proton-Induced Charge Transfer. *The Journal of Physical Chemistry A*, 122(6), 1634-1642.
- <sup>89</sup> Calvo, F., Bacchus-Montabonel, M. C., & Clavaguéra, C. (2016). Stepwise hydration of 2-aminooxazole: theoretical insight into the structure, finite temperature behavior and proton-induced charge transfer. *The Journal of Physical Chemistry A*, 120(15), 2380-2389.
- <sup>90</sup> Zins, E. L. (2020). Microhydration of a Carbonyl Group: How does the Molecular Electrostatic Potential (MESP) Impact the Formation of (H<sub>2</sub>O)  $n$ :(R<sub>2</sub>C=O) Complexes?. *The Journal of Physical Chemistry A*, 124(9), 1720-1734.
- <sup>91</sup> Kalai, C., Zins, E. L., & Alikhani, M. E. (2017). A theoretical investigation of water–solute interactions: from facial parallel to guest–host structures. *Theoretical Chemistry Accounts*, 136(4), 48.
- <sup>92</sup> Derbali, I., Thissen, R., Alcaraz, C., Romanzin, C., Zins, E. L.. Study of the reactivity of CH<sub>3</sub>COOH<sup>++</sup> and COOH<sup>+</sup> ions with CH<sub>3</sub>NH<sub>2</sub> : Evidence of the formation of new peptide C(O)-N bonds. Submitted for publication in the Journal of Physical Chemistry A.